Advances in Polymer Technology

Sustainable Bioproducts from Renewable Natural Polymers

Lead Guest Editor: Changlei Xia
Guest Editors: Ben-Hua Fei, Quyet Van Le, and Shengbo Ge

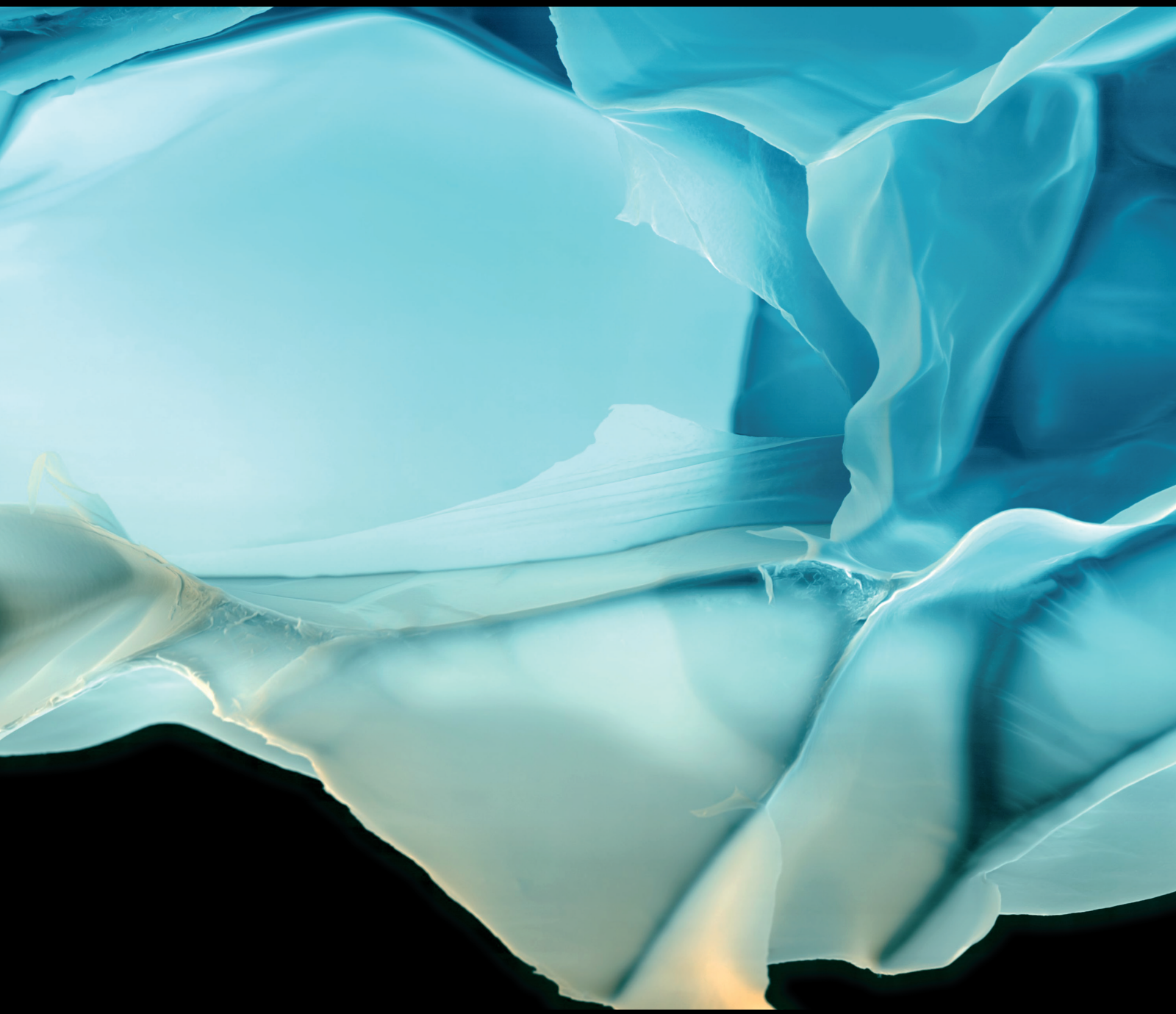

Sustainable Bioproducts from Renewable Natural Polymers

Advances in Polymer Technology

Sustainable Bioproducts from Renewable Natural Polymers

Lead Guest Editor: Changlei Xia
Guest Editors: Ben-Hua Fei, Quyet Van Le, and Shengbo Ge

Contents

Hindawi
Advances in Polymer Technology
Volume 2022, Article ID 5258130, 11 pages
https://doi.org/10.1155/2022/5258130

Research Article

Production and Characterization of Maximum Liquid Oil Products through Individual and Copyrolysis of Pressed Neem Oil Cake and Waste Thermocol Mixture

P. Madhu,[1] **M. Sasireka**,[2] **Ravi Samikannu**,[3] **K. Vinoth**,[4] **A. Udhaya Kumar**,[5] **Pravin P. Patil**,[6] **S. Kaliappan**,[7] **and Atkilt Mulu Gebrekidan**[8]

[1]*Department of Mechanical Engineering, Karpagam College of Engineering, Coimbatore, Tamilnadu, 641032, India*
[2]*Department of Electronics and Instrumentation Engineering, Kongu Engineering College, Perundurai, Tamilnadu, 638060, India*
[3]*Department of Electrical Computer and Telecommunications Engineering, Faculty of Engineering and Technology, Botswana International University of Science and Technology, Private Bag-16, Palapye, Botswana*
[4]*Department of Electrical and Electronics Engineering, Vel Tech Rangarajan Dr. Sagunthala R&D Institute of Science and Technology, Chennai, Tamilnadu, 600062, India*
[5]*Department of Electrical and Electronics Engineering, M.Kumarasamy College of Engineering, Karur, Tamilnadu, 639113, India*
[6]*Department of Mechanical Engineering, Graphic Era Deemed to be University, Bell Road, Clement Town Dehradun, Uttarakhand, 248002, India*
[7]*Department of Mechanical Engineering, Velammal Institute of Technology, Chennai, Tamilnadu, 601204, India*
[8]*Faculty of Mechanical Engineering, Arba Minch Institute of Technology, Arba Minch University, P.O. Box 21, Arba Minch, Ethiopia*

Correspondence should be addressed to Atkilt Mulu Gebrekidan; atkilt.mulu@amu.edu.et

Received 16 February 2022; Revised 9 April 2022; Accepted 18 April 2022; Published 5 May 2022

Academic Editor: Quyet Van Le

In this study, individual and copyrolysis experiments were performed with pressed neem oil cake (NOC) and waste thermocol (WT) to produce high grade liquid oil. The effects of reactor temperature, heating rate, feed ratio, and reaction time on product yields were investigated to identify the optimum parameters for maximum oil yield. The maximum oil yield of 49.3 wt%, 73.4 wt% and 88.5 wt% was obtained from NOC pyrolysis, copyrolysis, and WT pyrolysis under optimized conditions. During copyrolysis, the maximum oil product was obtained under NOC/WT ratio of 1 : 2 and at the temperature of 550°C. The liquid oils obtained from thermal and copyrolysis were subjected to detailed physicochemical analysis. When compared to biomass pyrolysis, the copyrolysis of WT and NOC had a substantial improvement in oil properties. The copyrolysis oil shows higher heating value of 40.3 MJ/kg with reduced water content. In addition to that, the copyrolysis oil obtained under optimized conditions is analyzed with Fourier transform infrared spectroscopy (FT-IR) and Gas chromatography–mass spectrometry (GC-MS) analysis to determine the chemical characterization. The analysis showed the presence of aliphatic and aromatic hydrocarbons in the oil.

1. Introduction

The need for energy in developing countries due to population growth leads to a shortage of resources. The necessity of renewable energy sources and efficient technologies for converting renewable sources into alternative fuels has now been recognized by the scientific community [1]. As a result, solar, hydro, wind, and biomass play an essential role in increasing renewable energy security with reduced pollution. The utilization of low polluting fuels like biomass has attracted more attention nowadays [2]. Furthermore, by 2035, biomass sources have the potential to contribute about 10% of global total energy consumption and biofuels will account for approximately 27% of global transportation fuels

[3]. Biomass is a potential source that is now being used in all energy sectors to replace fossil fuels. Agricultural residues are the kind of biomass from which valuable chemical elements and energy rich fuels can be extorted by various thermochemical conversion processes [4]. Biomass has many advantages, including low sulphur content and zero CO_2 emissions during recycling [5]. Various physical, chemical, and biological conversion processes are used to transform biomass into liquid, solid, and gaseous biofuel [6]. The main reason for biomass utilized for energy recovery is due to its low cost, year round availability, and higher conversion efficiency. Biofuels, in general, make no contribution towards CO_2 accumulation in the atmosphere [7].

Plastics are used for a variety of applications and are growing more popular every year as a result of their various advantages. But recycling and disposal are the two main disadvantages and are challengeable. Disposal and conversion of solid plastic waste are complicated one for most developing countries [8]. Plastics in various forms, such as low density polyethylene, polyethylene terephthalate, polyvinyl chloride, and polystyrene, are mostly produced for single use and accumulate in the world in huge volumes. They are waste commodity plastics becoming more prevalent. They dissolve slowly in the soil and contaminate it. So it should not be disposed of through the land filling method. They are not biodegradable, and it takes more than 400 years to break them down [9]. Currently, less than 9% of total plastic waste is physically recycled, 12% is burned, and the remainder ends up in landfills and the oceans [10]. It is a transparent material, but sometimes colourants can be added to it to make it colourful. It is thermally resistant, light in weight, inexpensive, and strong, making it suitable for a variety of applications. It is generally called polystyrene or thermocol which is recyclable and comes in two different types, such as expanded and solid.

The two possible sources for the production of alternative fuels are biomass and waste polymers. Pyrolysis, hydropyrolysis, and catalytic cracking are the common techniques used for the conversion of wastes into valuable fuels. Among other thermochemical conversion techniques, pyrolysis is a hopeful option due to its ease of operation and higher oil yield [11]. It is a thermal degradation process of feedstocks in which the biopolymers are broken down at elevated temperature in an oxygen-deficient environment to generate energy rich liquids, charcoal, and gaseous products [12]. Reactor temperature, pretreatment of the raw material, particle size, and heating rate of the reaction had an impact on the yield of the biofuel produced during pyrolysis. At lower temperature (<300°C), higher solids are formed. The breakdown of the existing glycosidic linkages in the polysaccharide structures generates mixes of levoglucosan, anhydrides, and oligosaccharides when the pyrolysis temperature is 300–450°C. Acetaldehyde, glyoxal, and acrolein chemicals are generated when the pyrolysis process is performed at temperatures more than 450°C [13]. Biofuel from biomass can be obtained through catalytic and noncatalytic processes. The components obtained from these processes are a combination of acids, alcohols, and phenols. Hydrocarbon in the oil can be obtained through synergistic effect and thermal cracking of biomass [14]. According to this study, the oil product obtained through the pyrolysis of palm oil empty fruit bunch can be considered an energy rich alternative fuel. Biofuels produced by biomass pyrolysis have some drawbacks, including higher oxygen content, poor heating value, and corrosive in nature. Pyrolysis of biomass combined with polymer is an efficient way for the production of energy rich synthetic liquid fuel by increasing the feedstock's total H/Ceff [15]. It could adjust carbon, hydrogen, and oxygen content prominent to positive synergistic effects. Jatropha, Mahua, Karanja, Sorghum, and Kusum are the dedicated energy plants widely available in India for the production of biofuels. These plants are generally grown all over the world. The benefits of pyrolysis of different oil seed cakes have been reported in several studies [16–18]. A huge amount of solid waste is produced every year as pressed oil cake, which is the outcome of the oil industries.

Azadirachta indica is a versatile medicinal plant with a broad range of biological activities. It is commonly called as neem tree and is cultivated in every part of the Indian subcontinent. All parts of the tree have been utilized as traditional medicine for household remedies against a variety of human illnesses [19]. The neem seed has a maximum oil content of 40–50% by weight and is primarily used to produce almost 3.5 lakhs tonnes of oil every year [20]. Neem oil is usually used for various medicinal purposes, and part of it is used for the production of biodiesel through various chemical processes. NOC is considered an imperative agro industrial by-product of the oil industry and is available in plenty. The WT utilized in this study is expanded polystyrene, which is widely manufactured across the world and used in a variety of purposes, including packaging, disposable cups, and insulators. However, once recycled, expanded polystyrene foam waste loses its foam qualities. It is feasible to re-gas recovered polystyrene, but this increases the cost of the product compared to virgin material [21]. The majority of WT trash is disposed by land filling, which is not environmentally friendly because WT is not biodegradable [22]. The copyrolysis of biomaterial with polymer is simple, cost-effective, and produces high-quality liquid products [23]. When compared to individual pyrolysis, the copyrolysis process yields more oil due to its synergistic effect [24]. Many researchers have investigated the copyrolysis of many polymeric materials with various biomass [25]. Shadangi and Mohanty [26] used a fixed bed reactor to copyrolyze Karanja and Niger seeds with thermocol under a 2 : 1 blending ratio to generate maximum oil with improved heating value. Mohapatra and Singh [27] examined the effects of process parameters and blending ratio on product yield by utilizing sugarcane bagasse and waste thermocol. When compared to biomass pyrolysis oil, the copyrolysis oil has a higher heating value, carbon, and hydrogen content [28].

To the best of the authors' knowledge, no study has been published on the pyrolysis of NOC blended with WT to produce pyrolysis oil. The aim of this study is to explore the pyrolysis technique as an effective and ecologically responsible way to dispose of WT along with NOC by transferring them into value-added compounds. In this study, experiments were conducted under different temperature, heating

rate, and blending ratios to investigate the effects on end products. With the aim of utilizing polymeric materials with biomass for the production of energy rich biofuel, WT pellets were mixed with NOC under different blending ratios. The pyrolysis oil obtained from thermal and copyrolysis was subjected to a detailed physicochemical analysis. In addition to that, a detailed chemical analysis was done on copyrolysis oil to identify the various chemical compounds present in the oil. The results obtained in this study offer a fundamental understanding of WT pyrolysis and present a novel waste reduction and hazard mitigation strategy.

2. Materials and Methods

The pressed neem cakes were collected from local oil mills located in Coimbatore, India. In order to remove the traces of oil and moisture, the material was dried in direct sunlight for one week. The WT sheets were collected from a local vendor. Before conducting pyrolysis experiments, NOC were cleaned carefully. After cleaning, they were air dried in the sunlight for a week. The material was further milled in a ball mill to prepare it for further analysis. In order to prepare for proximate and component analyses, the material was dried in an oven maintained at ±100°C for 45 minutes. The NOC used for pyrolysis was maintained at 0.5 to 1.0 mm. WT used for this study was heated at ±120°C for 60 min in an oven and then powdered using a hammer mill. NOC and WT granules were stored in airtight polythene containers until they were used for a further study.

2.1. Characterization. The proximate analyses of the selected feedstocks were performed in accordance with ASTM standards. The concentrations of carbon, hydrogen, nitrogen, and sulphur were analyzed using an Elementar Vario EL-III analyzer. The difference between the total compositions was used to determine the oxygen concentration of the samples. The heating value of the materials was calculated by Dulong using equations (1) and (2) proposed by Madhu et al. [29].

$$\mathrm{HHV_{dry}\,(MJ/kg)} = \frac{338.2\,x\,C + 1442.8\,x\,(H - (O/8))}{1000}, \quad (1)$$

$$\mathrm{LHV_{dry}(MJ/kg)} = \mathrm{HHV} - (0.218\,x\,H). \quad (2)$$

The BRUKER Optik FT-IR spectrometer was employed to identify the functional groups of the oil sample. The spectroscopy collected the spectral with the range of 500–4000cm^{-1}. A THERMO GC-TRACE ULTRA VER: 5.0, equipped with a THERMO MS DSQ-II analyzer, was used for the analysis of total chemical elements. The temperature of the column was initially set at 70°C and then increased to 300°C at a rate of 15°C/min. The spectra in this study were collected at 40-650m/z.

2.2. Experimental Setup. The pyrolysis and copyrolysis experiments were conducted in a stainless steel tubular reactor (L: 15 cm, ID: 10 cm). The reactor was heated electrically and insulated perfectly using mineral wool and Chromel-Alumel. The temperature of the reactor was controlled by PID a controller and measured with the help of thermocouples fixed at two different points within the reactor. The condenser unit was connected with sufficient ice water maintained at 5°C. For each run, the reactor was packed with 50 g of feedstock. The evolved gas condensed at the condenser was collected and stored in a borosilicate bottle. In order to separate the oil from the aqueous phase, the collected liquid was centrifuged at 3000 rpm. Figure 1 shows the reactor used for the study.

2.3. Experimental Procedure. In this study, three different series of tests were carried out. In the first series, the pyrolysis of NOC was performed to identify the optimum pyrolysis temperature for maximum oil yield by changing the reactor temperature from 350 to 550°C. The temperature range selected for this analysis was based on the thermal decomposition behavior of NOC obtained through TGA analysis. A maximum weight loss of 75.5% was obtained at temperatures ranging from 350 to 550°C. The next set of tests deals with determining the effect of heating rate on the pyrolysis yield of the NOC sample by varying the heating rate from 10 to 40°C/min. In the third series, the copyrolysis experiments on NOC and WT were performed (1 : 1 ratio) by keeping the reactor temperature at 500°C with 20°C/min heating rate. The fourth set of readings was taken by varying the blend ratios of NOC : WT as 1 : 0, 2 : 1, 1 : 1, 1 : 2, and 0 : 1 at 550°C. These experiments are also conducted at 20°C/min heating rate. To collect the condensable vapours, the condenser was attached to a flask. The amount of char that remained was also found. The material balance method was utilized to determine the weight of noncondensable gas products.

$$\text{Oil yield (wt\%)} = \frac{\text{Amount ofoil}}{\text{Total feed}}, \quad (3)$$

$$\text{Char yield (wt\%)} = \frac{\text{Amount of char}}{\text{Total feed}}, \quad (4)$$

$$\text{Gas yield (wt\%)} = 100 - (\text{oil yield} + \text{char yield}). \quad (5)$$

3. Results and Discussion

3.1. Feedstock Characterization. The results of proximate and component analysis of NOC and WT samples are presented in Table 1. From the analysis, it is evident that the selected material contains a large amount of volatiles, which gives anticipation for the production of higher liquid oil. The total hydrocarbon content for NOC is found to be 56.89 wt% with H/C and O/C ratio of 1.21 and 0.577, respectively. The heating value of the NOC is found to be 17.92 MJ/kg which is nearer to pressed rubber seed oil cake (19.58 MJ/kg) [30], rapeseed oil cake (19.49 MJ/kg) [31], and sesame oil cake (19.78 MJ/kg) [32]. The presence of ash in NOC is found to be lower (5.32 wt%) than *Madhuca Indica* oil cake (14.63 wt%), Jatropha oil cake (8.07 wt%), *Pongamia pinnata* oil cake (10.17 wt%) [33] and rubber seed oil cake [30].

3.2. Thermogravimetric Analysis of NOC and WT. The results of TGA analysis are shown in Figure 2 which shows the weight loss curves of NOC and WT. The curve shows

Figure 1: Reactor setup.

Table 1: Feedstock characteristics.

Parameters	NOC	WT
Proximate analysis in wt%		
Volatile matter	78.25	98.18
Fixed carbon	8.91	0.49
Moisture content	7.52	0.24
Ash	5.32	1.09
Ultimate analysis in wt%		
Carbon	51.62	89.2
Hydrogen	5.27	8.82
Nitrogen	3.1	0.01
Oxygen[a]	39.7	1.97
Sulphur	0.31	—
H/C ratio	1.21	1.10
O/C ratio	0.577	0.37
Empirical formula	$CH_{1.21}N_{0.05}O_{0.57}$	$CH_{1.10}N_{9.79}O_{0.03}$
Heating value in MJ/kg	17.92	40.49

[a]By difference.

the thermal degradation curves of the feedstock materials heated at 10°C/min. The results reveal that the total breakdown of the biomass takes place primarily in three stages: moisture removal, devolatilization, and char formation. 10% of mass loss occurred at temperatures up to 250°C, which reflects the evaporation of moisture content and low molecular weight components. A considerable portion of NOC (65 wt%) disintegrated in three stages between 250°C and 450°C, owing to predominantly cellulose and hemicellulose decompositions. The conversion of NOC into carbon residue occurs in the last stage at 500°C to 700°C. The decomposition of lignin causes around 15% of the mass loss at this stage. After 500°C, the material exhibits steady straight line degradation, indicating lignin breakdown, and this is referred to as passive pyrolysis. For WT, the structure is not as complicated as biomass. The curve revealed that considerable mass loss was found in a single phase [34]. The figure shows the deterioration of WT begins at 370°C and ends around at 500°C, with considerable weight loss of 96%, which is referred to as active pyrolysis zone. At 700°C, the residual mass was found to be 2 wt% and the result was verified with other reports [35, 36].

3.3. Pyrolysis Behavior of NOC. According to the TGA profile, the active pyrolysis of NOC takes place between 200°C and 550°C. As a result, NOC pyrolysis was conducted at the active pyrolysis temperature of 350°C to 550°C with 50°C temperature interval. Process temperatures and heating rates were investigated for their impact on product yield and quality.

3.3.1. Influence of Pyrolysis Temperature. The results for the first series of experiments are given in Figure 3. The tests were conducted on a fixed temperature of 350 to 550°C. By increasing the reactor temperature, the char products decreased but the gas yield increased, indicating that pyrolysis continued faster at a higher temperature. However, the gas yield did not change much until the temperature reached 500°C. At 500°C, the higher oil production of 46.6 wt% was recorded. The TGA curve shown in Figure 2 can be used to explain the declining trend of oil yield with respect to temperature. Around 375°C, the breakdown of hemicelluloses and cellulose is completed, as shown in the TGA curve. The breakdown of lignin is promoted at higher temperature, yielding the majority of char [37]. It is due to the fact that the rate of generation of condensable products by lignin breakdown is slower than the rate of breaking of condensable products into noncondensable gases above 500°C. Hence, the yield of noncondensable gas products reached maximum after 500°C. According to the findings, the oil yield increased from 31.4 wt% to 46.6 wt% when the temperature is increased from 350°C to 500°C. Beyond 500°C, the yield decreased to 42.5 wt%. It is also confirmed with the previous studies [38, 39]. With increasing pyrolysis temperature, a continuous decrement of char yield was recorded. The yield was 46.1 w% at 350°C and reduced to 25.0 wt% at 550°C. The total time for complete reaction was dropped from 66 minutes at 350°C to 34 minutes at 550°C, showing that higher temperature releases more volatiles in short duration [40].

3.3.2. Influence of Heating Rate. The pyrolysis yield of NOC with respect to heating rate is revealed in Figure 4. The results showed a reduction in char from 31.9 wt% to 28.4 wt% when the heating rate was increased from 10 to 40°C/min. However, increasing the heating rate from 10 to 20°C/min increases the oil production from 48.1 to 49.3 wt%. The yield of oil is further reduced with the increase of heating rate from 49.3 wt% (20°C/min) to 45.7 wt% (40°C/min). At higher heating, the yield of gas was high (25.9 wt%) and low at 10°C/min (20.0 wt%). The increased gas yield with a reduction in char at a higher heating rate is the effect of rapid depolymerization of solid components and the production of noncondensable gases during rapid heating [41]. With an increased heating rate, the total time required for a complete reaction was decreased from 51 minutes to 30 minutes. From Figure 4, it is clearly understood that the maximum oil product of 49.3 wt% was obtained from NOC at an optimum process temperature of 500°C and at 20°C/

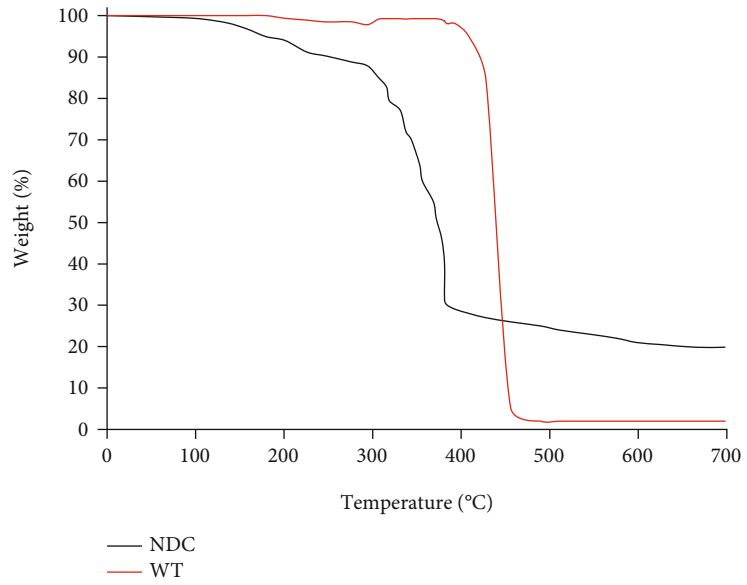

Figure 2: TGA thermogram of NOC and WT.

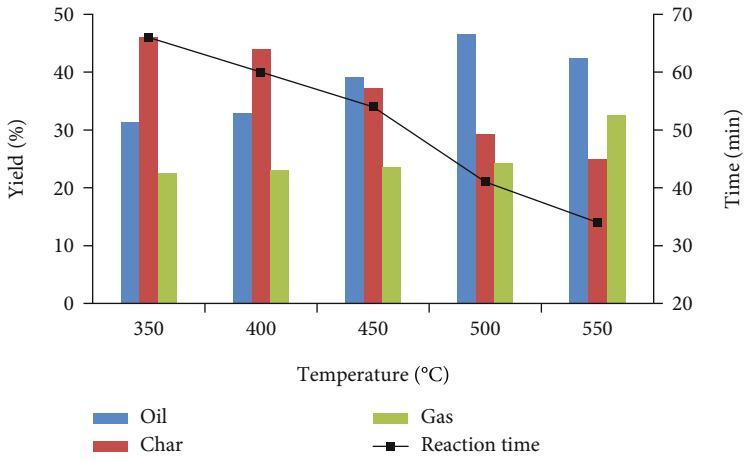

Figure 3: Effect of temperature on yields of NOC thermal pyrolysis.

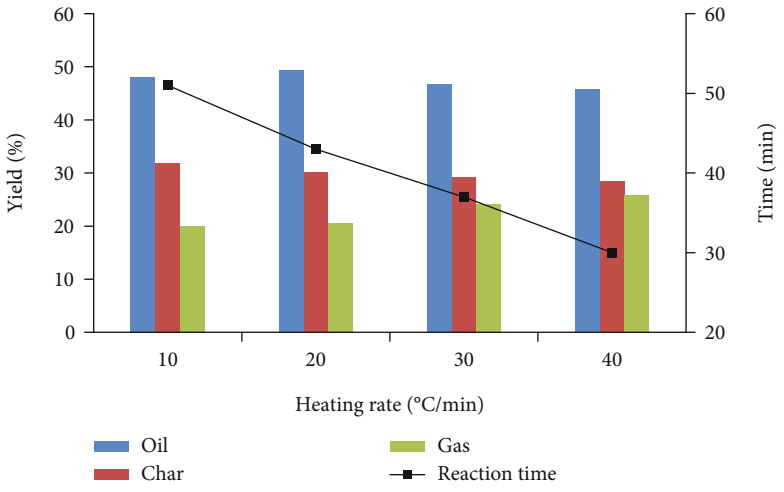

Figure 4: Effect of heating rate on yields of NOC thermal pyrolysis.

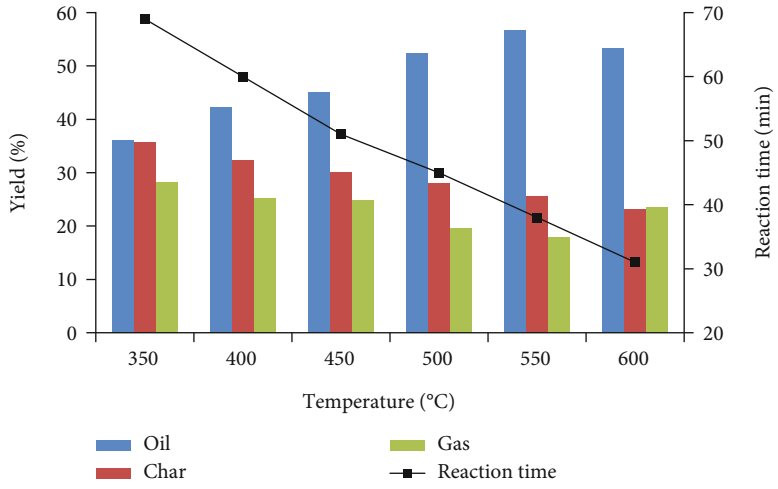

Figure 5: Effect of temperature on yields of WT thermal pyrolysis.

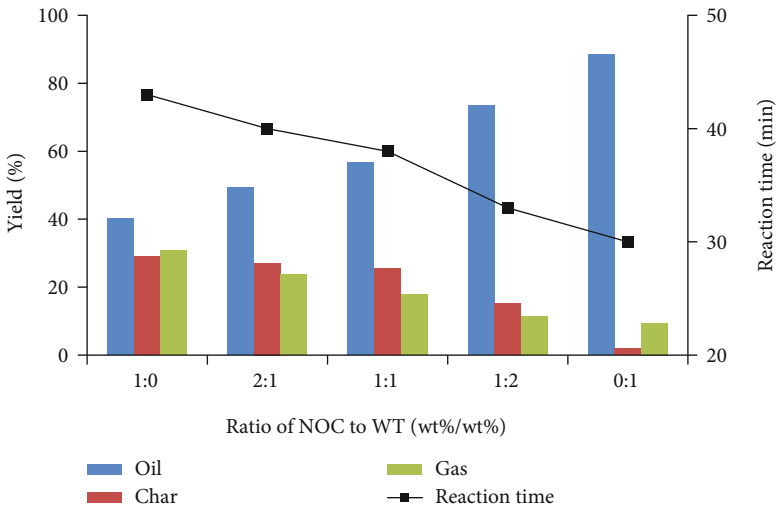

Figure 6: Effect of blending ratio on copyrolysis.

min heating rate. Based on the results, the copyrolysis characteristics were conducted by keeping the reactor at fixed temperate under 20°C/min heating rate.

3.4. Copyrolysis with Waste Thermocol. In order to find the possible improvements in pyrolysis product yields and properties, copyrolysis of NOC and WT was performed at 1 : 1 ratio. Figure 5 depicts the influence of reactor temperature on WT pyrolysis. Up to 550°C, there was possible increment in oil yield and decrement in char and gas yield. The char and gas products reduced from 35.7 wt% and 28.2 wt% to 25.6 wt% and 17.8 wt% with increased temperature from 350 to 550°C. The maximum oil production is recorded at a temperature of 550°C. Further increments in temperature reduce oil yield with increased gas fractions. The decrement in oil yield is endorsed by the increment in gas products. The increased oil yield is mostly attributable to the synergistic effect of NOC and WT owing to radical interaction [42]. Several studies have also reported that the highest temperature for copyrolysis is 550°C [43, 44]. Based on this result, the copyrolysis of NOC and WT was conducted at 550°C by varying the blending ratios of 1 : 0, 2 : 1, 1 : 1, 1 : 2, and 0 : 1 at 20°C/min.

3.5. Effect of Blending Ratio. Figure 6 shows the effect of addition of WT blend with NOC on the pyrolysis reaction. The copyrolysis experiments were conducted at the optimum conditions mentioned previously. In order to access the production distributions at different blendings, the blending ratio of NOC to WT was changed as: 1 : 0, 2 : 1, 1 : 1, 1 : 2, and 0 : 1. The addition of WT with biomass enhanced the yield of oil from 40.2 wt% (1 : 0 ratio) to 73.4 wt% (1 : 2 ratio). The gas and char yield from the smaller ratio were found to be 30.8 wt% and 29.0 wt%, respectively. Similar results were reported for sugarcane bagasse, rubber cake, palm shell, and Karanja blending with waste thermocol [26, 27, 29]. The aromatic content in WT attributed to a synergistic effect leads to maximum oil production. Furthermore, it is endorsed for the

Table 2: Comparison of oil properties.

Properties	NOC pyrolysis oil	Copyrolysis oil	WT pyrolysis oil	Diesel
Density	1105	1005	995	780 at 15°C
Viscosity at 40°C	13.1	4.28	4.14	13–3.3 at 50°C
Flash point	112	72	69	75
pH	4.2	4.4	4.4	—
Water content (wt%)	21.5	2.0	—	—

Table 3: Copyrolysis oil properties obtained at different blending ratios.

Items	Ratio of NOC to WT					Diesel
	1 : 0	2 : 1	1 : 1	1 : 2	0 : 1	
C	70.04	74.3	77.3	80	83.5	84-87
H	7.3	7.9	8.2	9.5	10.3	11-15
N	0.62	0.59	0.41	0.34	0.28	0.01-0.03
S	0.03	0.03	0.02	0.01	0	—
O	22.01	17.18	14.07	10.15	5.92	—
H/C	1.241	1.266	1.264	1.414	1.469	—
O/C	0.235	0.173	0.136	0.095	0.053	—
Empirical formula	$CH_{1.24}N_{0.007}O_{0.23}$	$CH_{1.26}N_{0.006}O_{0.17}$	$CH_{1.26}N_{0.004}O_{0.013}$	$CH_{1.41}N_{0.003}O_{0.09}$	$CH_{1.46}N_{0.002}O_{0.053}$	—
Heating value in MJ/kg	30.4	37.6	38.3	40.3	42.0	45-46

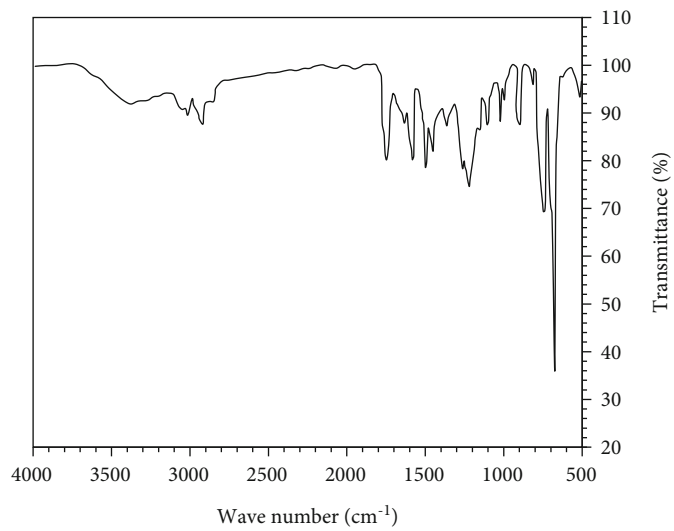

Figure 7: FT-IR analysis of copyrolysis oil.

transfer of hydrogen molecules from WT to biomass to produce maximum oil products [45]. From Figure 6, it is clearly visible that the maximum oil product of 73.4 wt% was obtained at 1 : 2 blend ratio and 88.5 wt% of oil was obtained from the thermal pyrolysis of WT.

3.6. Characterization Study

3.6.1. Physical Properties. The properties of individual and copyrolysis liquid oil acquired from NOC and WT (1 : 2 ratio) are displayed in Table 2. The results showed had better characteristics on copyrolysis oil than NOC thermal oil. Biomass derived liquid oil contains water contents, but the copyrolysis oil was water-free. This indicates that the copyrolysis process showed improved water and soluble chemical separation from the oil/organic phase. The viscosity was decreased to 4.28 cSt, and the value is proportional to the addition of WT. There is no major difference on pH value recorded for both oil. The density of the copyrolysis oil related to the spray pattern was found to be reduced to 1005 kg/m^3.

The heating values of raw NOC oil, WT oil, and copyrolysis oil were compared with diesel and reported in Table 3. The copyrolysis oils obtained under all blending ratios have

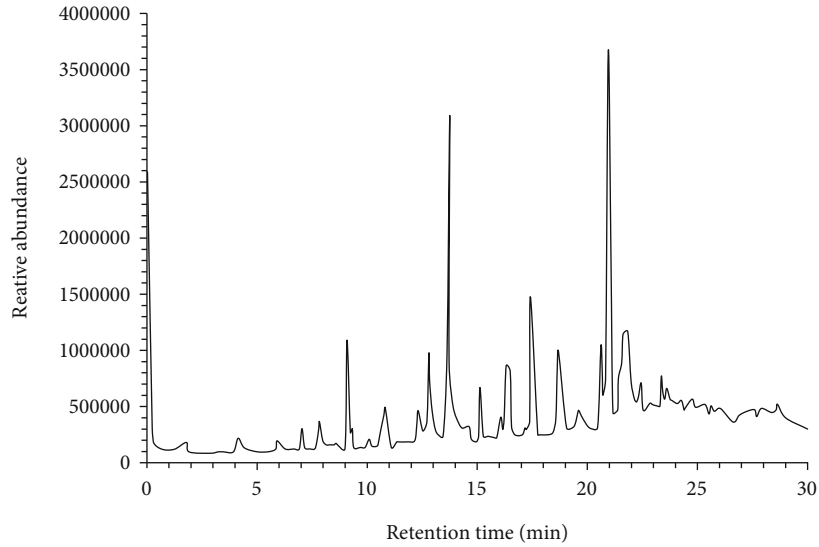

Figure 8: GC-MS spectrometry chromatograms of the copyrolysis oil.

Table 4: GC-MS analysis of the copyrolysis oil.

RT/min	Name of the compound	Molecular formula	Molecular weight	Area %
3.79	Pyridine	C_5H_5N	79	1.43
7.04	Phenol, 2,4-dimethyl-	$C_8H_{10}O$	122	1.92
9.08	Hentriacontane	$C_{31}H_{64}$	436	1.33
10.76	Benzene,1,4,9-decatrienyl-	$C_{16}H_{20}$	212	0.76
12.80	Toluene	C_7H_8	92	1.41
12.83	Benzene, (1-methylethyl)-	C_9H_{12}	120	5.28
13.75	2,4-Hexadiyne	C_6H_6	78	13.44
13.79	Acetonitrile, (m-phenoxyphenyl)-	$C_{14}H_{11}NO$	209	6.22
16.31	Cis-1-chloro-9-octadecene	$C_{18}H_{35}Cl$	286	0.53
17.41	1-Propene, 2-(2-methylphenyl)-1- phenyl-, (z)	$C_{10}H_{12}$	208	14.51
17.93	1,2-Diphenylcyclopropane	$C_{15}H_{14}$	194	2.02
18.63	Benzene, (2-methoxy-2-propenyl)-	$C_{10}H_{12}O$	148	0.33
18.91	4-Methyl-1,2-benzenediol	C_7H_8O	196	2.2
19.06	2-Cyclopenten-1-one, 2-hydroxy-3-methy	C_6H_8O	248	0.18
20.61	Furfural	$C_5H_4O_2$	96	10.82
20.70	cis-3-Methyl-3-hexene	C_7H_{14}	210	1.02
20.99	Carbonic acid, ethyl heptadecyl ester	$C_{27}H_{54}O_3$	328	0.11
21.34	Carbamic acid, ethylidenebis-, diethyl ester	$C_8H_{16}N_2O$	204	4.45
21.40	N-Propyl 9,12-octadecadienoate	$C_{21}H_{38}O_2$	322	4.92
21.55	Benzamide, N,N-dinonyl-4-butyl-	$C_{16}H_{25}NO$	428	3.52
21.67	Acetic acid, mercapto-, methyl ester	$C_3H_6O_2S$	106	9.23
21.83	1,4:3,6-Dianhydro-α-d-glucopyranose	$C_6H_8O_4$	144	5.54
22.9	Benzaldehyde, 4-hydroxy-3,5-dimethoxy-	$C_9H_{10}O$	194	1.85
23.15	1,2-benzenedicarboxylic acid	C_8H_6O	429	1.41
23.92	2-Cyclopenten-1-one, 2-methyl-	C_6H_8O	96	2.07
24.20	Phenol, 2-methyl-	C_7H_8O	108	1.35
24.72	2-ethylbutanal	$C_6H_{12}O$	375	1.04
25.06	N-(2-bromobenzoyl)-, pentyl ester	$C_{15}H_{20}BrNO_3$	340	0.54
25.91	4-Undecene, (z)-	$C_{11}H_{22}$	154	0.43
28.36	2,2-dimethyl-4-hexen-3-one	$C_8H_{14}O$	196	0.11

higher heating values than the biomass pyrolysis oil. The value is increased with respect to the increased polymer ratio. The result indicates that the oil produced at a 1 : 2 blend ratio has a higher heating value than other blends. The heating value of the WT pyrolysis oil (42.0 MJ/kg) is very near to diesel fuel. The increased heating value of the heavy pyrolysis oil was determined by the higher carbon content than the lighter oil [46]. The carbon content of the NOC pyrolysis oil was 70.04% offering a lower heating value of 30.4 MJ/kg whereas the value of carbon content was increased to 83.5% for WT pyrolysis oil, leading to a higher heating value of 42.0 MJ/kg.

3.6.2. FT-IR Analysis. The spectrum of copyrolysis oil found in FT-IR analysis is shown in Figure 7. The liquid oil made from the mixture of NOC and WT at 1 : 2 ratio was found to have the majority of aliphatic hydrocarbons. The presence of alkenes and alkanes in the oil sample was found by the absorption peaks identified between 3100 and 2850 cm^{-1}. The C=O stretch vibration between 1670 and 1820 cm^{-1} revealed the occurrence of oxygen, indicating a carbonyl group. The O-H stretch vibration concerning 3600 and 3200 cm^{-1} and C-O stretching vibration between 1300 and 1000 cm^{-1} recognized the occurrence of alcohols and esters. C=C stretching, which represents aromatic compounds, was detected between 1600 and 1400 cm^{-1}. C-H bending vibrations in the range of 900–690 cm^{-1} indicate the presence of aromatic hydrocarbons or arenes.

3.6.3. GC-MS Analysis. The GC-MS analysis of the copyrolysis oil is revealed in Figure 8. The aqueous phase in the tested sample was separated before the analysis, and the solid particles were separated by centrifuging at 3000 rpm for 15 minutes. The organic compounds were identified with respect to increased retention time. The total compounds identified in this study are reported in Table 4. The decreased oxygen content in pyrolysis oil might be related to deoxygenation reactions [47]. The oil contains the majority of aromatic groups of compounds, acids, and esters. Benzene, toluene, styrene, and some low molecular weight hydrocarbons and aromatic compounds were generated through the pyrolysis of oil cake with thermocol wastes [48]. The presence of these compounds is the cause of the increased heating value. At lower temperature (200–280°C) the lignocellulosic content in NOC degrades first to form acidic chemicals such as acetic acid [47]. According to the literature [49–51], phenols and its derivatives appeared in the pyrolysis oil are evidently due to the degradation of lignin in the NOC. According to Foong et al. [52], the lignin in the biomass material is converted into phenolic compounds through dehydration, depolymerization, and decarboxylation. Analysis of copyrolysis oil obtained at 1 : 2 blend ratio showed lower phenolic compounds than biomass pyrolysis oil [30, 52]. This is due to the addition of polymeric material to the biomass. The low amount of ketone, furan, styrene, and nitrogenated compounds leads to the oil becoming lighter. The copyrolysis process has altered the total composition of oil with increased hydrocarbon and abridged the formation of unfavourable chemical compounds with a higher heating value [26]. Similar observations are also made from the previously published literature [48, 53]. The findings of this study revealed that when WT was pyrolyzed with NOC the composition of the oil was totally altered.

4. Conclusion

Waste thermocol pellets were combined with pressed neem cake at various blending ratios with the aim of utilizing polymeric materials with biomass for the production of energy-dense liquid oil. This study investigated some selected process parameters for producing maximum oil through individual and copyrolysis processes. According to thermogravimetric study, the decomposition of biomass material can be roughly classified into moisture evaporation and active pyrolysis zones. By optimizing the various process parameters, a maximum oil yield of 49.3 wt%, 73.4 wt%, and 88.5 w% was obtained from individual NOC pyrolysis, copyrolysis, and individual WT pyrolysis. During individual and copyrolysis, the reactor temperature and feed ratio were the leading parameters to determine the oil yield and quality. The heating rate was the least significant factor in this study when determining the product yield. During the copyrolysis process, the maximum oil was acquired with 1 : 2 (NOC/WT) blending ratio at 550°C under 20°C/min heating rate. The physical characteristics of the oil obtained through the copyrolysis process at optimized conditions showed a higher heating value of 40.3 MJ/kg. The addition of WT to NOC increased the yield of pyrolysis oil from 40.2 to 88.5 wt% and the energy content from 30.4 to 42.0 MJ/kg. The heating values of the copyrolysis oils obtained at all blending ratios are higher than those of the biomass pyrolysis oil. The FT-IR and GC-MS reports of the copyrolysis oil show the presence of majority of aliphatic and aromatic hydrocarbons. Furthermore, this research suggests that copyrolysis might be a significant approach for proper waste management, particularly for the utilization of waste thermocol. Among the different compounds obtained through the copyrolysis process, the presence of maximum hydrocarbons is a valuable component which can be used as industrial chemical feedstock and fuel additives. This technology upgraded the waste-to-energy technologies for utilizing locally available low value biomass materials. To fulfill the need for fuel, further work may be extended to improve the oil yield by utilizing low-cost catalysts.

Data Availability

The data used to support the findings of this study are included within the article.

Conflicts of Interest

The authors declare that there is no conflict of interest regarding the publication of this article.

References

[1] R. A. Felseghi, E. Carcadea, M. S. Raboaca, C. N. Trufin, and C. Filote, "Hydrogen fuel cell technology for the sustainable future of stationary applications," *Energies*, vol. 12, no. 23, p. 4593, 2019.

[2] Z. Zou, L. Ju, B. Zhou et al., "Progress in microwave pyrolysis conversion of agricultural waste to value- added biofuels: a batch to continuous approach," *Renewable and Sustainable Energy Reviews*, vol. 135, article 110148, 2021.

[3] C. S. Dhanalakshmi, M. Mathew, and P. Madhu, "Biomass material selection for sustainable environment by the application of multi-objective optimization on the basis of ratio analysis (MOORA)," in *Materials, Design, and Manufacturing for Sustainable Environment*, pp. 345–354, Springer, Singapore, 2021.

[4] N. H. Nam, V. N. Linh, L. D. Dung, and V. T. T. Ha, "Physico-chemical characterization of forest and agricultural residues for energy conversion processes," *Vietnam Journal of Chemistry*, vol. 58, no. 6, pp. 735–741, 2020.

[5] Ş. Alayont, D. B. Kayan, H. Durak, E. K. Alayont, and S. Genel, "The role of acidic, alkaline and hydrothermal pretreatment on pyrolysis of wild mustard (Sinapis arvensis_) on the properties of bio-oil and bio-char," *Bioresource Technology Reports*, vol. 17, article 100980, 2022.

[6] H. Durak, "Characterization of products obtained from hydrothermal liquefaction of biomass (Anchusa azurea) compared to other thermochemical conversion methods," *Biomass Conversion and Biorefinery*, vol. 9, no. 2, pp. 459–470, 2019.

[7] M. I. Khan, J. H. Shin, and J. D. Kim, "The promising future of microalgae: current status, challenges, and optimization of a sustainable and renewable industry for biofuels, feed, and other products," *Microbial Cell Factories*, vol. 17, no. 1, pp. 1–21, 2018.

[8] K. R. Vanapalli, B. Samal, B. K. Dubey, and J. Bhattacharya, "Emissions and environmental burdens associated with plastic solid waste management," in *Plastics to Energy*, pp. 313–342, William Andrew Publishing, 2019.

[9] A. Chamas, H. Moon, J. Zheng et al., "Degradation rates of plastics in the environment," *ACS Sustainable Chemical Engineering*, vol. 8, no. 9, pp. 3494–3511, 2020.

[10] T. M. Letcher, "Introduction to plastic waste and recycling," in *Plastic Waste and Recycling*, pp. 3–12, Academic Press, 2020.

[11] I. Kathir, K. Haribabu, A. Kumar et al., "Utilization of tea industrial waste for low-grade energy recovery: optimization of liquid oil production and its characterization," *Advances in Materials Science and Engineering*, vol. 2022, Article ID 7852046, 2022.

[12] H. Durak, "Pyrolysis ofXanthium strumariumin a fixed bed reactor: effects of boron catalysts and pyrolysis parameters on product yields and character," *Energy Sources, Part A: Recovery, Utilization, and Environmental Effects*, vol. 38, no. 10, pp. 1400–1409, 2016.

[13] E. Yücedağ and H. Durak, "Bio-oil and bio-char from lactuca scariola: significance of catalyst and temperature for assessing yield and quality of pyrolysis," *Energy Sources, Part A: Recovery, Utilization, and Environmental Effects*, vol. 44, no. 1, pp. 1774–1787, 2022.

[14] S. Sunarno, R. P. Sari, T. Frimacia, S. R. Yenti, P. S. Utama, and E. Saputra, "Catalytic co-pyrolysis of palm oil empty fruit bunch and coal into liquid oil," *International Journal of Renewable Energy Development*, vol. 11, no. 2, pp. 463–469, 2022.

[15] K. G. Burra and A. K. Gupta, "Kinetics of synergistic effects in co-pyrolysis of biomass with plastic wastes," *Applied Energy*, vol. 220, pp. 408–418, 2018.

[16] M. Siva Sankari, S. Vivekanandhan, M. Misra, and A. K. Mohanty, "Oil cakes as sustainable agro-industrial feedstock for biocarbon materials," *ChemBioEng Reviews*, vol. 9, no. 1, pp. 21–41, 2022.

[17] P. Schroeder, B. P. do Nascimento, G. A. Romeiro, M. K. Figueiredo, and M. C. da Cunha Veloso, "Chemical and physical analysis of the liquid fractions from soursop seed cake obtained using slow pyrolysis conditions," *Journal of Analytical and Applied Pyrolysis*, vol. 124, pp. 161–174, 2017.

[18] A. Mohanty, P. R. Rout, B. Dubey, S. S. Meena, P. Pal, and M. Goel, "A critical review on biogas production from edible and non-edible oil cakes," *Biomass Conversion and Biorefinery*, pp. 1–18, 2021.

[19] S. C. Kiran, C. Nagarajaiah, K. T. Prasanna, and K. Rajeshkumar, "Studies on bioavailability of nutrients in decomposed crushed seeds, oil cakes and deoiled cakes of neem (Azadirachta indica L.)," *Journal of Pharmacognosy and Phytochemistry*, vol. 8, no. 2, pp. 163–165, 2019.

[20] L. A. M. Syndia, P. N. Prasad, G. Annadurai, R. R. Nair, S. Thilaga, and D. Ganesh, "Characterization of neem seed oil and de–oiled cake for its potentiality as a biofuel and biomanure," *Int. Res. J. Pharm. Biosci.*, vol. 2, pp. 10–19, 2015.

[21] I. M. Maafa, "Pyrolysis of polystyrene waste: a review," *Polymers*, vol. 13, no. 2, p. 225, 2021.

[22] S. S. Bag, A. Bora, and A. K. Golder, "Turning wastes into value-added materials: polystyrene nanocomposites (PS-AgNPs) from waste thermocol and green synthesized silver nanoparticles for water disinfection application," *Polymer Composites*, vol. 42, no. 11, pp. 6094–6105, 2021.

[23] H. Shafaghat, H. W. Lee, Y. F. Tsang et al., "In-situ_ and _ex-situ_ catalytic pyrolysis/co-pyrolysis of empty fruit bunches using mesostructured aluminosilicate catalysts," *Chemical Engineering Journal*, vol. 366, pp. 330–338, 2019.

[24] H. Hassan, B. H. Hameed, and J. K. Lim, "Co-pyrolysis of sugarcane bagasse and waste high-density polyethylene: synergistic effect and product distributions," *Energy*, vol. 191, article 116545, 2020.

[25] Z. Wang, K. G. Burra, T. Lei, and A. K. Gupta, "Co-pyrolysis of waste plastic and solid biomass for synergistic production of biofuels and chemicals-a review," *Progress in Energy and Combustion Science*, vol. 84, article 100899, 2021.

[26] K. P. Shadangi and K. Mohanty, "Co-pyrolysis of Karanja and Niger seeds with waste polystyrene to produce liquid fuel," *Fuel*, vol. 153, pp. 492–498, 2015.

[27] S. S. Mohapatra and R. K. Singh, "Production and characterization of the maximum liquid product obtained from co-pyrolysis of sugarcane bagasse and thermocol waste," *Cellulose*, vol. 28, no. 7, pp. 4223–4239, 2021.

[28] G. Hu, J. Li, X. Zhang, and Y. Li, "Investigation of waste biomass co-pyrolysis with petroleum sludge using a response surface methodology," *Journal of Environmental Management*, vol. 192, pp. 234–242, 2017.

[29] P. Madhu, H. Kanagasabapathy, and I. N. Manickam, "Cotton shell utilization as a source of biomass energy for bio-oil by flash pyrolysis on electrically heated fluidized bed reactor,"

Journal of Material Cycles and Waste Management, vol. 18, no. 1, pp. 146–155, 2016.

[30] A. S. Reshad, P. Tiwari, and V. V. Goud, "Thermal and co-pyrolysis of rubber seed cake with waste polystyrene for bio-oil production," *Journal of Analytical and Applied Pyrolysis*, vol. 139, pp. 333–343, 2019.

[31] S. Ucar and A. R. Ozkan, "Characterization of products from the pyrolysis of rapeseed oil cake," *Bioresource Technology*, vol. 99, no. 18, pp. 8771–8776, 2008.

[32] V. Volli and R. K. Singh, "Production of bio-oil from de-oiled cakes by thermal pyrolysis," *Fuel*, vol. 96, pp. 579–585, 2012.

[33] R. Gottipati and S. Mishra, "A kinetic study on pyrolysis and combustion characteristics of oil cakes: effect of cellulose and lignin content," *Journal of Fuel Chemistry and Technology*, vol. 39, no. 4, pp. 265–270, 2011.

[34] I. Dubdub and M. Al-Yaari, "Pyrolysis of low density polyethylene: kinetic study using TGA data and ANN prediction," *Polymers*, vol. 12, no. 4, p. 891, 2020.

[35] J. Nisar, G. Ali, A. Shah et al., "Fuel production from waste polystyrene via pyrolysis: kinetics and products distribution," *Waste Management*, vol. 88, pp. 236–247, 2019.

[36] G. Özsin, A. E. Pütün, and E. Pütün, "Investigating the interactions between lignocellulosic biomass and synthetic polymers during co-pyrolysis by simultaneous thermal and spectroscopic methods," *Biomass Conversion and Biorefinery*, vol. 9, no. 3, pp. 593–608, 2019.

[37] C. Sowmya Dhanalakshmi and P. Madhu, "Utilization possibilities ofAlbizia amaraas a source of biomass energy for bio-oil in pyrolysis process," *Energy Sources, Part A: Recovery, Utilization, and Environmental Effects*, vol. 41, no. 15, pp. 1908–1919, 2019.

[38] S. Thirugnanam, R. Srinivasan, K. Anand et al., "Utilisation possibilities of waste medium-density fiberboard: a material recycling process," *Materials Today: Proceedings.*, 2021.

[39] Y. Fan, Y. Xiong, W. Zhao, L. Jin, and Y. Chen, "Process optimization and stability characterization of the bio-oil produced from vacuum pyrolysis ofrape straw," *Energy Sources, Part A: Recovery, Utilization, and Environmental Effects*, vol. 43, no. 13, pp. 1649–1659, 2021.

[40] R. Serefentse, W. Ruwona, G. Danha, and E. Muzenda, "A review of the desulphurization methods used for pyrolysis oil," *Procedia Manufacturing*, vol. 35, pp. 762–768, 2019.

[41] R. S. Chutia, R. Kataki, and T. Bhaskar, "Characterization of liquid and solid product from pyrolysis of _Pongamia glabra_ deoiled cake," *Bioresource Technology*, vol. 165, pp. 336–342, 2014.

[42] N. I. Izzatie, M. H. Basha, Y. Uemura et al., "Co-Pyrolysis of Rice Straw and Polypropylene Using Fixed-Bed Pyrolyzer," in *IOP Conference Series: Materials Science and Engineering*, vol. 160, no. 1p. 012033, IOP Publishing, 2016.

[43] O. Sanahuja-Parejo, A. Veses, M. V. Navarro et al., "Drop-in biofuels from the co-pyrolysis of grape seeds and polystyrene," *Chemical Engineering Journal*, vol. 377, article 120246, 2019.

[44] S. Sharma, V. Dutta, and M. Eswaramoorthy, "An experimental investigation on multi-V and protrusion element on absorber plate of solar air heater," *Energy Sources, Part A: Recovery, Utilization, and Environmental Effects*, vol. 42, no. 22, pp. 2742–2750, 2020.

[45] Q. Van Nguyen, Y. S. Choi, S. K. Choi, Y. W. Jeong, and Y. S. Kwon, "Improvement of bio-crude oil properties via co-pyrolysis of pine sawdust and waste polystyrene foam," *Journal of Environmental Management*, vol. 237, pp. 24–29, 2019.

[46] H. Durak and S. Genel, "Characterization of bio-oil and bio-char obtained from black cumin seed by hydrothermal liquefaction: investigation of potential as an energy source," *Energy Sources, Part A: Recovery, Utilization, and Environmental Effects*, vol. 1-11, pp. 1–11, 2020.

[47] T. Aysu and H. Durak, "Catalytic pyrolysis of liquorice (_Glycyrrhiza glabra_L.) in a fixed-bed reactor: effects of pyrolysis parameters on product yields and character," *Journal of Analytical and Applied Pyrolysis*, vol. 111, pp. 156–172, 2015.

[48] A. Veses, O. Sanahuja-Parejo, M. V. Navarro et al., "From laboratory scale to pilot plant: evaluation of the catalytic co-pyrolysis of grape seeds and polystyrene wastes with CaO," *Catalysis Today*, vol. 379, pp. 87–95, 2021.

[49] H. Durak, "Hydrothermal liquefaction of Glycyrrhiza glabra L.(Liquorice): effects of catalyst on variety compounds and chromatographic characterization," *Energy Sources, Part A: Recovery, Utilization, and Environmental Effects*, vol. 42, no. 20, pp. 2471–2484, 2020.

[50] C. S. Dhanalakshmi and P. Madhu, "Recycling of wood bark of Azadirachta indica for bio-oil and chemicals by flash pyrolysis," *Indian Journal of Ecology*, vol. 46, no. 2, pp. 347–353, 2019.

[51] C. Vibhakar, R. S. Sabeenian, S. Kaliappan et al., "Production and Optimization of Energy Rich Biofuel through Co-Pyrolysis by Utilizing Mixed Agricultural Residues and Mixed Waste Plastics," *Advances in Materials Science and Engineering*, vol. 2022, Article ID 8175552, 2022.

[52] S. Y. Foong, R. K. Liew, C. L. Lee et al., "Strategic hazard mitigation of waste furniture boards via pyrolysis: pyrolysis behavior, mechanisms, and value-added products," *Journal of Hazardous Materials*, vol. 421, article 126774, 2022.

[53] M. Sarker and M. M. Rashid, "Waste plastics mixture of polystyrene and polypropylene into light grade fuel using Fe_2O_3 catalyst," *Int. J. Renew. Energy Technol. Res*, vol. 2, no. 1, pp. 17–28, 2013.

Hindawi
Advances in Polymer Technology
Volume 2022, Article ID 6547461, 9 pages
https://doi.org/10.1155/2022/6547461

Research Article

Development of Starch-Based Bioplastic from Jackfruit Seed

Trieu Khoa Nguyen, Nguyen Thy Ton That, Nien Thi Nguyen, and Ha Thi Nguyen

Faculty of Mechanical Engineering, Industrial University of Ho Chi Minh City, Ho Chi Minh City 70000, Vietnam

Correspondence should be addressed to Trieu Khoa Nguyen; nguyenkhoatrieu@iuh.edu.vn

Received 29 January 2022; Revised 4 March 2022; Accepted 10 March 2022; Published 26 March 2022

Academic Editor: Changlei Xia

In this article, jackfruit seed starch plasticized with common plasticizers was developed and characterized. At the first step, the research papers that dealt with the fabrication and characterization of starch-based bioplastics were synthesized and analyzed. Next, jackfruit seeds were selected as a source for starch because of their large availability, low price or even free, and high starch capacity. Afterward, a starch-based bioplastic fabrication procedure was proposed. From preliminary tests, plasticizers were sufficiently selected, including water, glycerol, natri bicarbonate, and acid citric. Using different combinations of these plasticizers, four types of bioplastics were then fabricated to study the effect of the plasticizers as well as to characterize the properties of the corresponding bioplastics. A cutting tool for ASTM D412 type A standard tensile testing specimen was then designed and fabricated. Using these dog-bone specimens, tensile results showed that the hardness of the fabricated bioplastic was positively proportional to the ratio of the starch. Furthermore, from SEM characterization, the bioplastic specimens were fully plasticized. Although the fabricated bioplastic has lower mechanical properties than petroleum-based plastics, its environmental friendliness and high potential added value promise to be a material of the future.

1. Introduction

There has been an increasing interest in the production of bioplastics as the environmental pollution from conventional plastics is increasingly evident [1–3]. The bioplastic industry is being considered in the world as the 4.0 revolution of green technology [1, 4]. Environmental pollution, especially pollution caused by plastic waste, is globally becoming more and more serious [5, 6]. Petroleum-derived plastics pollute the soil, water, and air. They could also destroy the habitats of many species, reduce biodiversity, cause many direct impacts on humans, and hence, is likely to result in the unsustainability of global development. Bioplastics, new environmentally friendly materials, are promised to be a great solution to replace traditional plastics, thereby contributing to reducing plastic waste pollution and protecting the living environment on earth.

Bioplastics can also be biobased (originated from renewable materials) and biodegradable (that can be back to nature). In terms of renewability and production, some of the most widely known biobased plastics nowadays are polylactic acid (PLA), starch-based plastics, protein-based plastics, cellulose esters, polyhydroxyalkanoates (PHAs) [1], and plant fibres [7, 8]. Bioplastics, manufactured from biomass, with or without modifications, such as starch, protein, and cellulose, are biodegradable and therefore gaining more and more attention. Among these, starch has shown potential for the fabrication of biodegradable materials as it is cheap, readily available, and renewable [2]. It should also be noted that, in addition to being used to produce bioplastics, biomass can also be used to produce biogas, biooil, biocoal [9], and bioethanol [10].

Bioplastics produce remarkably less greenhouse gas (carbon dioxide) emissions than traditional oil-based plastics over their lifetime [11]. Since the plants that biobased plastics are made from absorbed that same amount of greenhouse gas as they grew, there is no net increment in this gas. With such advantages, bioplastics have been studied a lot in the world, especially the production of bioplastics from starch. The authors in [12, 13] used rice starch and some plasticizers such as glycerol, sorbitol, and formamide to produce bioplastics. These authors chose rice starch because it contains a high amount of amylose, about 30%, which is suitable for coating materials. Furthermore, Taghizadeh and Favis [14] used wheat

starch to make plastic. Meanwhile, Thunwall et al. from Sweden [15], Talja et al. from Finland [16], and Ozdamar and Ates from Turkey [17] utilized potato starch to produce bioplastic because of its popularity. In addition, Niu et al. [18] utilized response surface methodology (RSM) combined with the multi-index comprehensive evaluation method to prepare and characterize biodegradable composited films using potato starch. Another starch, corn starch, in addition to fermentation to make PLA, was utilized by many authors to make bioplastics directly [19–21], mainly for packaging. Similarly, there have been many other authors using other starch sources such as sweet potato [22, 23], tapioca [24, 25], avocado seeds [26–28], jackfruit seed [2, 29, 30], and durian seed [31, 32]. In addition, many authors also utilized many types of starch blends to achieve bioplastics with better properties. For example, Lopattananon et al. from Thailand [33] used a mixture of tapioca and rice starch to make bioplastics, while Yin et al. [34] utilized oxidized wood pulp fiber to incorporate into thermoplastic starch (TPS) to prepare new composites. And Marichelvam et al. from India [35] mixed corn and rice starch to result in shorter biodegradation time bioplastics. The common feature of these studies was that the fabrication of bioplastics is based exclusively on starch which requires the supplement of plasticizers. Because these bioplastics had low machinability, they were difficult to adapt to the conventional processes. In addition, whatever the botanical origin, starch-based bioplastics showed a strong hydrophilic character, which made them unsatisfactory for several applications [2].

Although bioplastics are commonly considered to be more environmentally friendly than petroleum-based plastics, that is not necessarily the case when considering the life cycle of the materials [11]. Bioplastic fabrication processes result in a large number of pollutants, because of the fertilizers and pesticides utilized to grow the plants and the chemical processing needed to change organic materials to plastics [11]. While the biodegradability of bioplastics is regarded as an advantage, most bioplastics require high-temperature industrial facilities to be broken down. Very few countries have the necessary infrastructure to deal with this composting procedure. Hence, bioplastics usually end up in landfills where, due to being deprived of oxygen, they may release methane, a greenhouse gas, 23 times more harmful than carbon dioxide. Bioplastics are also relatively costly. Due to the complex processes utilized to turn corn starch or sugarcane into building blocks, PLA plastic can be 20 to 50 percent more high-priced than comparable plastic materials [11].

Therefore, the research on manufacturing, improving the useful properties, and using bioplastics in the world in general and in Vietnam, in particular, is very necessary. In this study, in order to exploit agricultural wastes, the bioplastic was made from the starch of jackfruit seeds. This is so because jackfruit seeds are common in Vietnam and easy to gather in large quantities, especially from those factories producing dried jackfruit. In addition, these seeds are also normally sold at a negligible price or even free of charge. After a starch extracting process, water, glycerol, natri bicarbonate, and acid citric were applied as plasticizers. The environmental friendliness and high-potential added value of the fabricated biopolymer promise to be a material of the future.

2. Materials and Methods

2.1. Materials

2.1.1. Jackfruit Seed. Jackfruit seeds were obtained from a very popular variety, called Changai—originating from Thailand, in the South of Vietnam. Analysis of the main components of jackfruit seeds detected the presence of $30.08\% \pm 0.1$ amylose [2] or $26.4\% \pm 0.7$ amylose in [36]; $7.16\% \pm 0.04$ moisture; $1.17\% \pm 0.03$ total protein; $0.3\% \pm 0.01$ lipids; $0.21\% \pm 0.03$ ash; and $0.15\% \pm 0.02$ fibers [2]. In the present study, it was important to consider the amount of ash, amylose, and lipid found as these components influenced the formation of bioplastics. A low percentage of ash was indicated by a low concentration of minerals in the jackfruit seed. Due to possible interactions between minerals with amylose, amylopectin, and plasticizers, the high concentration of these compounds interfered with the formation of bioplastics [2]. The found lipid percentage in jackfruit seed starch was low ($0.3\% \pm 0.01$). High lipid percentage in starch might affect the color of the bioplastics. Furthermore, lipids could negatively affect the water absorption stage of starch granules, change the plasticizing temperature, and limit the amylose retrogradation, and therefore, the bioplastic becomes brittle. In previous studies, 30.08% amylose was found in jackfruit seed starch, which could be considered as high amylose content [2]. The amylose content is an essential property for the formation of bioplastics because it is responsible for gelatinization and retrogradation process. In other words, amylose is responsible for hydrogen bonding between the hydroxyl groups of biopolymers that form intermolecular junctions and lead to film production. The physical, chemical, and functional properties of the fabricated bioplastics depend on the ratio between amylose and amylopectin [2].

2.1.2. Glycerol. A classical starch plasticizer is perhaps the thermoplastic starch's most commonly investigated and utilized plasticizer. This is due to its low price, nontoxicity for human food and biomedical applications, and relatively high boiling point (292°C). Furthermore, the hydrolysis or conversion of lipids (triglycerides) to fatty acids for the biodiesel industry produces glycerol as a by-product [1]. This presents an opportunity to improve the economics of both the biodiesel industry and the bioplastics industry.

2.1.3. Acid Citric. The adhesion between glycerol, water, citric acid, and starch in thermoplastic starch is strengthened by the supplementation of citric acid [37, 38]. Citric acid can create stronger hydrogen bonding interactions with starch than glycerol. Hence, citric acid can effectually inhibit starch recrystallization (i.e., retrogradation), due to its strong hydrogen bonding interaction with starch. Rheological investigations demonstrated that citric acid can clearly reduce the shear viscosity and improve the fluidity of thermoplastic starch. Citric acid can also enhance the elongation of glycerol-plasticized thermoplastic starch and improve its water resistance at high relative humidity, but reduce the tensile stress [37]. Citric acid and glycerol are utilized to enhance the flexibility and fluidity of the material

Table 1: The ratio of the raw material composition of plastic specimens.

Ingredients	Starch : glycerol	Citric acid : (starch+glycerol)	Baking soda : (starch+glycerol)	Starch : water
Ratio	3.50 : 1 3.00 : 1 2.75 : 1 2.50 : 1	1 : 100	5 : 100	12.5 : 100

Table 2: The specific weight of each material.

Specimens	Ingredients				
	Starch (g)	Glycerol (g)	Citric acid (g)	Baking soda (g)	Water (g)
Ratio 3.5 : 1	20	5.71	0.25	1.28	160
Ratio 3.0 : 1	20	6.67	0.26	1.33	160
Ratio 2.75 : 1	20	7.27	0.27	1.36	160
Ratio 2.5 : 1	20	8.00	0.28	1.40	160

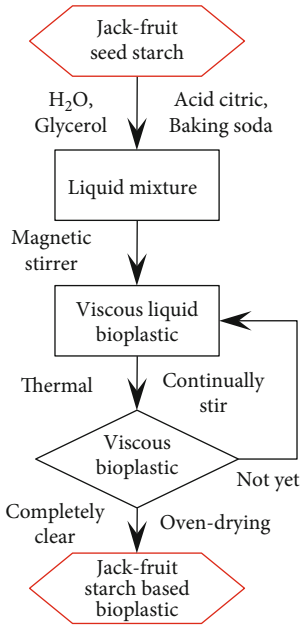

Figure 1: Flow diagram of bioplastic fabrication using jackfruit seed starch.

Figure 2: Flattened viscous bioplastic on the PE film coated tray.

to which they are supplemented. Furthermore, citric acid is a potential cross-linking agent under low-cost, nontoxic conditions.

2.1.4. Baking Soda. Baking soda, also known as sodium bicarbonate ($NaHCO_3$), scientifically, is one of the preservatives and plasticizer additives as the same as sodium metabisulfite ($Na_2S_2O_5$), glycerol, and sorbitol. These additions strengthen bioplastics and make them more durable [37].

2.2. Methods

2.2.1. Starch Extraction. First, starch was extracted to prepare raw materials for making bioplastics. The raw jackfruit seed has a very pungent odor and hard outer shell and then needs to be deseeded for both the hard shell and the brown spermoderm. The deseeded seeds were then washed. The rotten seeds were discarded while the good seeds were overnight soaked for latex removal. After that, the overnight soaked jackfruit seeds were washed using pure water. Clean jackfruit seeds were then ground to obtain a slurry. The slurry was filtered through a filter cloth to obtain a crude starch suspension while the sediment was discarded. The filtrate was precipitated overnight for settlement and latex and minerals removal. The supernatant was removed, and the crude starch was washed with distilled water. This step was reproduced three times [39], and the starch cake was then dried naturally or by an oven. When using the sun-drying method, starch could be discolored and became contaminated, forming a thin light brown layer. Instead, the starch suspension was dried at 45°C for 24 hours in an oven dryer. It should be added that the proposed starch extraction process is simple and easy to implement. It does not include a

(a) (b)

Figure 3: Drying stage. (a) Tray dryer with air circulation at a temperature of 55°C. (b) Dried bioplastic specimens.

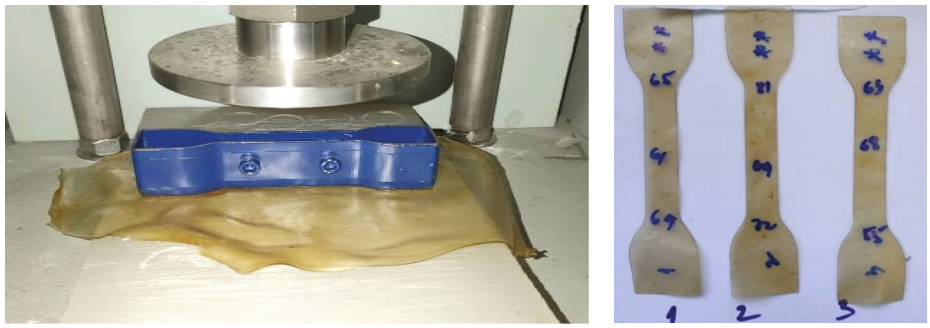

(a) (b)

Figure 4: Characterization for mechanical properties. (a) Stamping process for dog-bone samples. (b) Dog-bone samples for tensile testing.

centrifugation step as in [2], soaking in 2% NaOH and slicing as in [29], or cutting with the size of 1 cm^2 approximately before crushing as in [30].

2.2.2. Bioplastic Fabrication. After extracting starch, bioplastic was fabricated. The proportions of ingredients were selected for the production of bioplastics as shown in Table 1. These ratios were selected similarly to [24] for easy comparison of results. From there, the specific weight of each material was calculated as shown in Table 2.

Bioplastics are prepared by mixing starch with glycerol with different starch : glycerol ratios by mass (2.5 : 1; 2.75 : 1; 3.0 : 1; and 3.5 : 1) [2, 23] and by as shown in the flowchart in Figure 1. The plasticization process was carried out by putting the liquid mixture with the ingredients in a given ratio above a heated magnetic stirrer (SCILOGEX model MS-H-S) at a temperature of 95°C. The mixture was stirred with a magnetic stir bar. When the temperature is higher, the process will go faster; however, when the temperature is too high, the mixture can be thermally decomposed before being completely converted into bioplastic. After the mixture turned completely clear and thick, stop stirring. The plastic mixture was poured into trays covered with PE film (Figure 2). Without PE film coating, the bioplastic would stick to the tray and be cracked when drying. After that, the viscous liquid bioplastic was flattened on a tray (Figure 2) and then transferred to an oven at 55°C (Figure 3(a)) and dried for 15 hours until the weight was constant. A natural air circulation MEMMERT UNB400 universal oven was utilized for this step. It is worth noting that the drying time can be shorter or longer depending on the thickness of the viscous bioplastic layer. The dried bioplastic specimens are shown in Figure 3(b).

From the diagram in Figure 1, it can be observed that the proposed procedure is simple and suitable for laboratories at universities. According to the literature review, the shaking step in the ultrasonic bath [2] was eliminated. In addition, since pure starch is used, an additive blending step is also unnecessary both before and after plasticization as in [29, 30], respectively.

3. Results and Discussion

3.1. Mechanical Properties. Bioplastic specimens were stamped into dog-bone samples according to ASTM D412-Type A standard (Figures 4(a) and 4(b)). In this study, to measure the mechanical properties of bioplastic specimens, the U-CAN DYNATEX INC TYPE UT-2080 tensile tester (Figure 5(a))

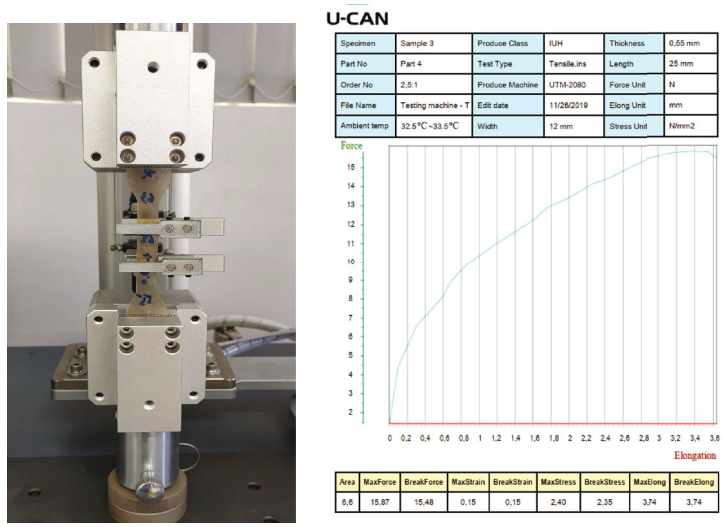

(a) (b)

Figure 5: Tensile strength testing stage. (a) Tensile strength tester. (b) A typical result of the tensile test of the bioplastic sample.

Table 3: Results of mechanical properties of bioplastics.

Results	Types			
	Ratio 2.5 : 1	Ratio 2.75 : 1	Ratio 3.0 : 1	Ratio 3.5 : 1
Max stress σ (MPa)	3.39	3.90	4.08	5.15
Strain ε	0.29	0.23	0.31	0.25
Young modulus E (MPa)	12.70	16.96	13.53	20.06
Elongation A (%)	29.13	22.60	30.67	25.20
Density (g/cm^3)	1.375	1.385	1.403	1.410

was used. The density of the samples was determined by an electronic densimeter MDS-300. Three dog-bone samples were used for the mechanical characterization of each type of bioplastic. A typical result of the tensile test of the bioplastic sample was shown in Figure 5(b).

The initial observation showed that the higher the glycerol ratio was, the softer and more flexible the bioplastic became, and vice versa. Increasing the percentage of citric acid enhanced the hardness and reduced the plasticity of the bioplastic. At the same time, if the flattened viscous biopolymer layer was made too thick, it would be cracked due to shrinkage.

Based on the measured results (Table 3) and the plot (Figure 6), in general, the mechanical properties of bioplastics increase gradually with the starch : glycerol ratio. However, in the sample with a ratio of 3 : 1, there was a difference. The reason might be that the air bubbles inside the bioplastic were not removed completely. This led to nonuniform mechanical measurement samples in terms of material distribution (more or less air bubbles inside), affecting the measurement results. In addition, another very important cause was the uneven thickness of the specimens due to the manual leveling of the viscous bioplastic in the tray before drying. The tensile fracture position might have a smaller thickness than the clamping position. Bioplastics with a ratio of 3.5 : 1 had the highest strength in this study but were still low compared to traditional petroleum-based plastics. Therefore, bioplastics from jackfruit seeds cannot replace traditional plastics in many fields of application that require high mechanical properties yet, as other common bioplastics [40]. However, compared with other bioplastics that have been studied, the results are encouraging. Also making bioplastics from jackfruit seed starch, the authors in [2] obtained the highest tensile strength of 3.12 MPa with 30% glycerol. As for the authors from Indonesia [23], they made bioplastic from sweet potato starch; a maximum tensile strength of 2.57 MPa with a starch/glycerol ratio of 3.5/1 could be obtained. In addition, the authors in [41] reported that the tensile strength of bioplastics made from potato starch reached 4.87 MPa, from tapioca starch reached 4.5 MPa, and from corn starch 3.59 MPa.

3.2. Scanning Electron Microscope (SEM) Characterization. The SEM characterization was performed using Hitachi scanning electron microscope S-4800. Figure 7(a) showed the morphology of jackfruit seed starch in this investigation. The jackfruit seed starch granules are varied round to bell shapes with smooth surfaces. Previous studies revealed that the granular size lied between 5 and 10 μm [42]. In our case, the average granular size is 8.2 μm as shown in Figure 7(a). Because of its small size, jackfruit seed starch granular can be a great source for encapsulated products [43]. Morphology and structure were firstly analyzed only for bioplastic specimens with a ratio of 2.5 : 1 (Figure 7(b)) and a ratio of 3.5 : 1 (Figure 7(d)). SEM photographs show that the surfaces exposed to air are rough. The micrographs do not illustrate any intact starch granules, which implies that the jackfruit starch was fully gelatinized during the forming of the film specimens. In addition, analyses of the bioplastic surfaces reveal that the specimen with a ratio of 3.5 : 1 has some microcrack on its surface. These microcracks occurred on the tougher specimen with a lower amount of glycerol.

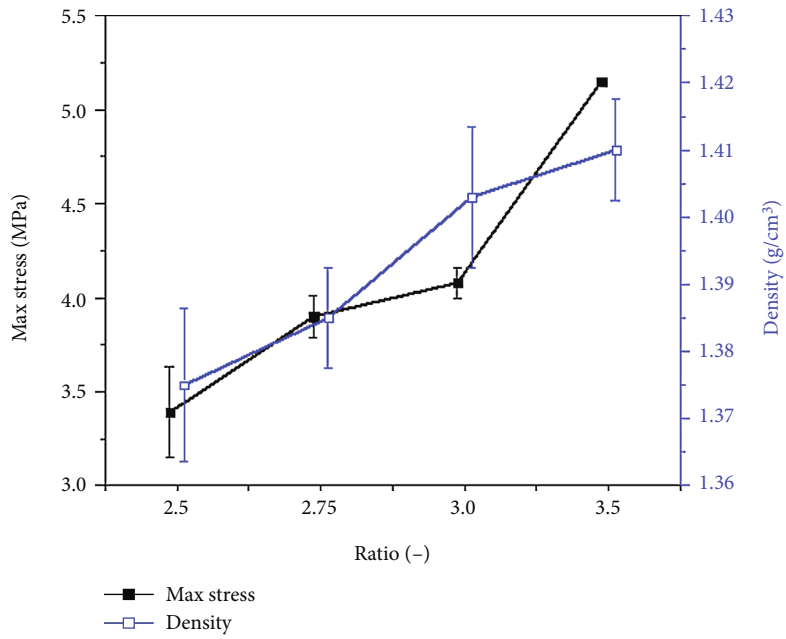

Figure 6: The plot of max stress and density for each type of bioplastic.

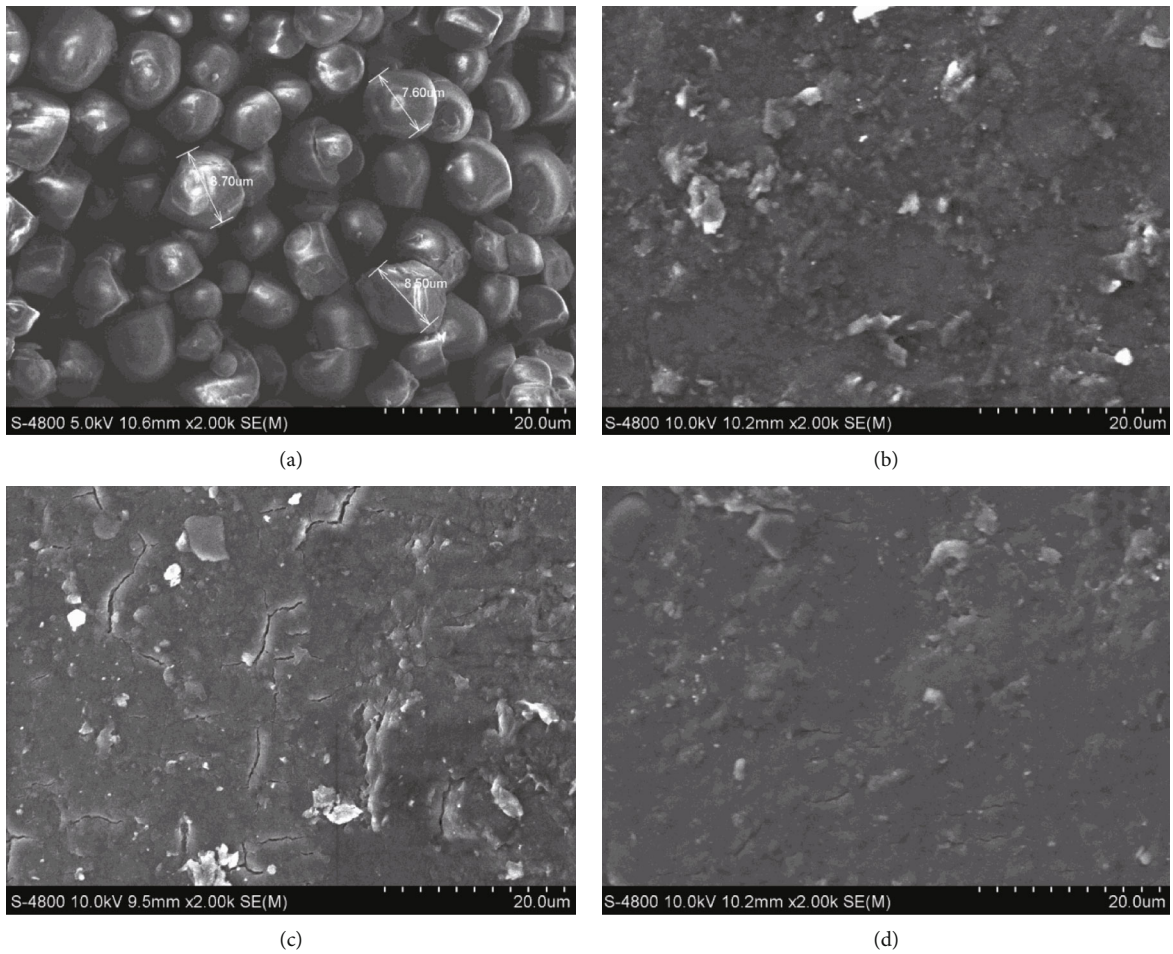

Figure 7: SEM characterization with 2000 times magnification. (a) Starch from jackfruit seed. (b) Bioplastic with ratio 2.5 : 1. (c) Bioplastic with ratio 3 : 1. (d) Bioplastic with ratio 3.5 : 1.

After that, an additional SEM analysis was done for the specimen with a ratio of 3 : 1 due to its special mechanical results. The SEM image in Figure 7(c) is in agreement with others on a full polymerization process. However, there were many microcracks on the surface of the specimen. The occurrence of these microcracks may be due to the presence of microbubbles formed during the gelatinization process [2]. These microbubbles were caused by hydrogen bonding chains of the starch, which began to break down when reaching the gelatinization temperature and the water molecules started to infiltrate into hydroxyl groups in the starch molecule [25]. Unfortunately, in this bioplastic production process, due to the lack of a vacuum step, the number of microbubbles in the specimens was uncontrollable. In addition, the microair bubbles generated by mixing and stirring could not be fully eliminated.

4. Conclusions

A review of the literature revealed that plastic pollution is becoming a burning issue worldwide. To overcome that problem, many measures have been studied. This paper presents a process for making an environmentally friendly bioplastic from jackfruit seed starch. Jackfruit seed has a high starch content (about 30% of fresh seed weight) and is easy to collect in large quantities and extract starch. Therefore, it is suitable as a raw material source for bioplastics and at the same time takes advantage of the source of fruit seeds that can be considered waste products, increasing the value of crops. When making the bioplastic, the strength was generally proportional to the ratio of starch : glycerol. From SEM characterization, bioplastic specimens were fully plasticized. However, an excessive amount of starch would cause incomplete plasticization, while a too low ratio would make bioplastics unable to harden after drying. Bioplastic with the ratio of 3.5 : 1 has the best tensile strength, 5.12 MPa according to our measurements. However, the mechanical properties of the bioplastics could be greater because the specimens still had microair bubbles inside; at the same time, the thickness was not uniform, affecting the measurement results.

From the encouraging results of this study, and the great potential of bioplastics, the next research topic is to build a jackfruit seed peeling machine and a centrifuge to facilitate the starch extraction process. In addition, a vacuum desiccator and vacuum pump will be used to remove microair bubbles before drying, to achieve more accurate measurement results. The time and decomposition of the bioplastic under the normal using conditions and in the natural environment also need to be studied precisely. After that, the plasticizing temperature will be studied to develop a lab-scale injection molding machine for the bioplastics. Products from bioplastics will be then researched and developed. In addition, the simple processes of starch extraction and bioplastic fabrication also promise that this proposed method can be applied to industrial production in the near future.

Data Availability

No data were used to support this study.

Conflicts of Interest

The authors declare that there is no conflict of interest regarding the publication of this paper.

Acknowledgments

The experiments were done by Huynh Thong Nguyen, Van Thuong Le, Thanh Van Tran, Van Vu Le (Faculty of Mechanical Engineering, Industrial University of Ho Chi Minh City, Ho Chi Minh City, Vietnam) under the supervision of Dr. Trieu Khoa Nguyen. The mechanical characterization of the bioplastics was performed at Quoc Huy Anh Corporation, which is the strategic partner and representative of Dow Corning Corporation (USA), Shinetsu (Japan), and April Group (Indonesia-Singapore). The SEM characterization of the bioplastics was carried out at the Research Laboratories of Saigon High Tech Park, District 9, HCMC.

References

[1] T. Mekonnen, P. Mussone, H. Khalil, and D. Bressler, "Progress in bio-based plastics and plasticizing modifications," *Journal of Materials Chemistry A*, vol. 1, no. 43, pp. 13379–13398, 2013.

[2] R. F. Santana, R. C. F. Bonomo, O. R. R. Gandolfi et al., "Characterization of starch-based bioplastics from jackfruit seed plasticized with glycerol," *Journal of Food Science and Technology*, vol. 55, no. 1, pp. 278–286, 2018.

[3] M. Ramesh, C. Deepa, L. R. Kumar, M. R. Sanjay, and S. Siengchin, "Life-cycle and environmental impact assessments on processing of plant fibres and its bio-composites: a critical review," *Journal of Industrial Textiles*, pp. 1–25, 2020.

[4] M. Rosseto, D. D. C. Krein, N. P. Balbé, and A. Dettmer, "Starch–gelatin film as an alternative to the use of plastics in agriculture: a review," *Journal of the Science of Food and Agriculture*, vol. 99, no. 15, pp. 6671–6679, 2019.

[5] W. Sikorska, M. Musioł, B. Zawidlak-Węgrzyńska, and J. Rydz, "End-of-life options for (bio)degradable polymers in the circular economy," *Advances in Polymer Technology*, vol. 2021, Article ID 6695140, 2021.

[6] I. N. Vikhareva, G. K. Aminova, A. I. Moguchev, and A. K. Mazitova, "The effect of a zinc-containing additive on the properties of PVC compounds," *Advances in Polymer Technology*, vol. 2021, Article ID 5593184, 2021.

[7] M. Ramesh, K. Palanikumar, and K. H. Reddy, "Plant fibre based bio-composites: sustainable and renewable green materials," *Renewable and Sustainable Energy Reviews*, vol. 79, pp. 558–584, 2017.

[8] M. Ramesh, L. Rajeshkumar, and V. Bhuvaneswari, "Leaf fibres as reinforcements in green composites: a review on processing, properties and applications," *Emergent Materials*, 2021.

[9] M. Esfandyari, A. Hafizi, and M. Piroozmand, "5-Production of biogas, bio-oil, and biocoal from biomass," in *Advances in Bioenergy and Microfluidic Applications*, M. R. Rahimpour, R. Kamali, M. A. Makarem, and M. K. D. Manshadi, Eds., Elsevier, 2021.

[10] A. Patel and A. R. Shah, "Integrated lignocellulosic biorefinery: gateway for production of second generation ethanol and

value added products," *Journal of Bioresources and Bioproducts*, vol. 6, no. 2, pp. 108–128, 2021.

[11] I. D. Posen, P. Jaramillo, A. E. Landis, and W. M. Griffin, "Greenhouse gas mitigation for U.S. plastics production: energy first, feedstocks later," *Environmental Research Letters*, vol. 12, no. 3, article 034024, 2017.

[12] N. Laohakunjit and A. Noomhorm, "Effect of plasticizers on mechanical and barrier properties of rice starch film," *Starch-Stärke*, vol. 56, no. 8, pp. 348–356, 2004.

[13] X. Ma and J. Yu, "Formamide as the plasticizer for thermoplastic starch," *Journal of Applied Polymer Science*, vol. 93, no. 4, pp. 1769–1773, 2004.

[14] A. Taghizadeh and B. D. Favis, "Effect of high molecular weight plasticizers on the gelatinization of starch under static and shear conditions," *Carbohydrate Polymers*, vol. 92, no. 2, pp. 1799–1808, 2013.

[15] M. Thunwall, A. Boldizar, M. Rigdahl, and V. Kuthanová, "On the stress-strain behavior of thermoplastic starch melts," *International Journal of Polymer Analysis and Characterization*, vol. 11, no. 6, pp. 419–428, 2006.

[16] R. A. Talja, H. Helén, Y. H. Roos, and K. Jouppila, "Effect of various polyols and polyol contents on physical and mechanical properties of potato starch-based films," *Carbohydrate Polymers*, vol. 67, no. 3, pp. 288–295, 2007.

[17] E. G. Özdamar and A. T. Murat, "Rethinking sustainability: a research on starch based bioplastic," *Journal of Sustainable Construction Materials and Technologies*, vol. 3, no. 3, pp. 249–260, 2018.

[18] X. Niu, Q. Ma, S. Li et al., "Preparation and characterization of biodegradable composited films based on potato starch/glycerol/gelatin," *Journal of Food Quality*, vol. 2021, Article ID 6633711, 2021.

[19] V. S. Keziah, R. Gayathri, and V. V. Priya, "Biodegradable plastic production from corn starch," *Drug Invention Today*, vol. 10, pp. 1315–1317, 2018.

[20] J. F. Mendes, R. T. Paschoalin, V. B. Carmona et al., "Biodegradable polymer blends based on corn starch and thermoplastic chitosan processed by extrusion," *Carbohydrate Polymers*, vol. 137, pp. 452–458, 2016.

[21] O. V. López, C. J. Lecot, N. E. Zaritzky, and M. A. García, "Biodegradable packages development from starch based heat sealable films," *Journal of Food Engineering*, vol. 105, no. 2, pp. 254–263, 2011.

[22] E. U. Offiong and S. L. Ayodele, "Preparation and characterization of thermoplastic starch from sweet potato," *International Journal of Scientific & Engineering Research*, vol. 7, pp. 438–443, 2016.

[23] A. H. D. Abdullah, S. Pudjiraharti, M. Karina, O. D. Putri, and R. H. Fauziyyah, "Fabrication and characterization of sweet potato starch-based bioplastics plasticized with glycerol," *Journal of Biological Sciences*, vol. 19, pp. 57–64, 2019.

[24] O. Udensi, E. V. Ikpeme, E. A. Uyoh, and E. A. Brisibe, "Evaluation of starch biodegradable plastics derived from cassava and their rates of degradation in soil," *Nigerian Journal of Biotechnology*, vol. 20, pp. 28–33, 2009.

[25] N. E. Wahyuningtiyas and H. Suryanto, "Analysis of biodegradation of bioplastics made of cassava starch," *Journal of Mechanical Engineering Science and Technology*, vol. 1, no. 1, pp. 24–31, 2017.

[26] M. H. S. Ginting, R. Hasibuan, M. Lubis, F. Alanjani, F. A. Winoto, and R. C. Siregar, "Supply of avocado starch (Persea americana mill) as bioplastic material," *IOP Conference Series: Materials Science and Engineering*, vol. 309, article 012098, 2018.

[27] M. Lubis, M. B. Harahap, M. H. S. Ginting, M. Sartika, and H. Azmi, "Production of bioplastic from avocado seed starch reinforced with microcrystalline cellulose from sugar palm fibers," *Journal of Engineering Science and Technology*, vol. 13, pp. 381–393, 2018.

[28] R. Ramesh, H. Palanivel, S. Venkatesa Prabhu, B. Z. Tizazu, and A. A. Woldesemayat, "Process development for edible film preparation using avocado seed starch: response surface modeling and analysis for water-vapor permeability," *Advances in Materials Science and Engineering*, vol. 2021, Article ID 7859658, 2021.

[29] A. W. M. Kahar, M. Lingeswarran, M. Z. Amirah Hulwani, and H. Ismail, "Plasticized jackfruit seed starch: a viable alternative for the partial replacement of petroleum-based polymer blends," *Polymer Bulletin*, vol. 76, no. 2, pp. 747–762, 2019.

[30] M. B. Maulida, A. Harahap, A. Manullang, and M. H. S. Ginting, "Utilization of jackfruit seeds (Artocarpus heterophyllus) in the preparing of bioplastics by plasticizer ethylene glycol," *ARPN Journal of Engineering and Applied Sciences*, vol. 13, pp. 240–244, 2018.

[31] W. Pimpa, C. Pimpa, and P. Junsangsree, "Development of biodegradable films based on durian seed starch," *Advanced Materials Research*, vol. 506, pp. 311–314, 2012.

[32] M. H. S. Ginting, R. Hasibuan, M. Lubis, D. S. Tanjung, and N. Iqbal, "Effect of hydrochloric acid concentration as chitosan solvent on mechanical properties of bioplastics from durian seed starch (Durio Zibethinus) with filler chitosan and plasticizer sorbitol," *IOP Conference Series: Materials Science and Engineering*, vol. 180, article 012126, 2017.

[33] N. Lopattananon, C. Thongpin, and N. Sombatsompop, "Bioplastics from blends of cassava and rice flours: the effect of blend composition," *International Polymer Processing*, vol. 27, no. 3, pp. 334–340, 2012.

[34] P. Yin, W. Zhou, X. Dong, B. Guo, and Y. Huang, "Effect of oxidized wood pulp fibers on the performance of the thermoplastic corn starch composites," *Advances in Polymer Technology*, vol. 2020, Article ID 8976713, 2020.

[35] K. M. Marichelvam, M. Jawaid, and M. Asim, "Corn and rice starch-based bio-plastics as alternative packaging materials," *Fibers*, vol. 7, no. 4, p. 32, 2019.

[36] O. S. Kittipongpatana and N. Kittipongpatana, "Resistant starch contents of native and heat-moisture treated jackfruit seed starch," *The Scientific World Journal*, vol. 2015, Article ID 519854, 2015.

[37] Y. Jiugao, W. Ning, and M. Xiaofei, "The effects of citric acid on the properties of thermoplastic starch plasticized by glycerol," *Starch - Stärke*, vol. 57, no. 10, pp. 494–504, 2005.

[38] J. Wang, M. Euring, K. Ostendorf, and K. Zhang, "Biobased materials for food packaging," *Journal of Bioresources and Bioproducts*, vol. 7, pp. 1–13, 2022.

[39] F. Noor, "Physicochemical properties of flour and extraction of starch from jack-fruit seed," *International Journal of Nutrition and Food Sciences*, vol. 3, no. 4, p. 347, 2014.

[40] H. C. Oyeoka, C. M. Ewulonu, I. C. Nwuzor, C. M. Obele, and J. T. Nwabanne, "Packaging and degradability properties of polyvinyl alcohol/gelatin nanocomposite films filled water hyacinth cellulose nanocrystals," *Journal of Bioresources and Bioproducts*, vol. 6, no. 2, pp. 168–185, 2021.

[41] M. S. Rahmatiah Al Faruqy and K. C. Liew, "Properties of bioplastic sheets made from different types of starch incorporated with recycled newspaper pulp," *Materials Science - Transactions on Science and Technology*, vol. 3, pp. 257–264, 2016.

[42] D. Kaur, R. Kushwaha, and V. Singh, "Comprehensive review of the impact of modification on the properties of jack-fruit seed starch and its applications," *Nutrafoods*, vol. 1, pp. 68–79, 2019.

[43] N. S. M. Yazid, N. Abdullah, and N. Muhammad, "Comparison of chemical, functional and morphological characteristics of jack-fruit (Artocarpus heterophyllus Lam.) (J33) seed starch and commercial native starches," *IOP Conference Series: Earth Environment Sciences*, vol. 269, no. 1, article 012031, 2019.

Hindawi
Advances in Polymer Technology
Volume 2022, Article ID 9999339, 8 pages
https://doi.org/10.1155/2022/9999339

Research Article

Laminarin Alleviates the Ischemia/Reperfusion Injury in PC12 Cells via Regulation of PTEN/PI3K/AKT Pathway

Zhishan Sun,[1,2] Honghai Wang,[3] Wenwen Zhao,[4] and Dehui Wang[1,2]

[1]*Department of Neurosurgery, Weifang People's Hospital, Weifang 261041, China*
[2]*Department of Neurosurgery, Weifang Brain Hospital, Weifang 261021, China*
[3]*Department of Neurology, Weifang People's Hospital, Weifang 261041, China*
[4]*Department of Urology, Affiliated Hospital of Weifang Medical University, Weifang 261101, China*

Correspondence should be addressed to Dehui Wang; wangdehui370725@163.com

Received 22 December 2021; Revised 1 March 2022; Accepted 7 March 2022; Published 18 March 2022

Academic Editor: Changlei Xia

Objective. To investigate the protective effect of laminarin on PC12 cells damaged by oxygen glucose deprivation/reoxygenation (OGD/R) and its molecular mechanism. *Methods*. PC12 cells in the logarithmic phase were randomly divided into the control group, OGD/R group, and OGD/R+laminarin (0.5, 2.5, and 5 μg/ml) group. CCK-8 activity assay kit was used to detect cell viability. ELISA kit was performed to examine the levels of proinflammatory factors (TNF-α, IL-1β, and IL-6) and oxidative stress markers (ROS, LDH, and MPO). In addition, flow cytometry was employed to determine cell cycle and apoptosis. The expression of cell proliferation-related proteins (PCNA and Ki67), apoptosis-related proteins (Bcl-2, Bax, and Caspase-3), and PTEN/PI3K/AKT pathway-related proteins was evaluated by Western blot. *Results*. Compared with the control group, the cell viability was decreased significantly in the OGD/R group. CCK-8 results showed that laminarin could attenuate the damage of PC12 cell viability induced by OGD/R in a concentration-dependent manner. Meanwhile, the highest concentration of 5 μg/ml laminarin could significantly promote the viability of PC12 cells and the expression of PCNA and Ki67 than the OGD/R group. Additionally, ELISA assays showed that laminarin significantly inhibited the expression of proinflammatory factors (TNF-α, IL-1β, and IL-6) and the levels of oxidative stress markers (ROS, LDH, and MPO). Flow cytometry results demonstrated that laminarin promoted the cell cycle. And laminin upregulated the expression of apoptotic protein Bcl-2, while downregulated the expression of apoptotic proteins Bax and Caspase-3. Finally, laminarin significantly suppressed the expression of PTEN and facilitated the expression of PI3K and p-AKT compared to the OGD/R group. *Conclusion*. Laminarin could alleviate the OGD/R-induced PC12 cell neuronal injury via promoting cell activity and cycle and inhibiting inflammation, oxidative stress, and apoptosis. The mechanism may be related to the downregulation of PTEN protein and the activation of the PI3K/AKT pathway.

1. Introduction

Ischemic stroke is an acute cerebrovascular disease that can seriously affect patients' quality of life [1, 2]. According to statistics, about 1.5 million people die of ischemic stroke in China every year. More importantly, the disease was the first cause of death in China in 2017 [3]. Studies have shown that stroke patients will have a sustained brain injury due to insufficient oxygen and glucose supply in the brain. There is no effective treatment at present. Clinically, stroke patients mainly recover the blood supply of ischemic brain tissue as soon as possible through thrombolysis to alleviate symptoms. However, limited perfusion time window and rapid blood perfusion will lead to further pathological damage of ischemic tissue, namely, hypoxia reperfusion (OGD/R) injury [4, 5]. Studies have confirmed that neuronal OGD/R injury is a complex physiological process involving reactive oxygen species (ROS), proinflammatory mediators, and apoptotic genes [6]. Therefore, it is imperative to develop new neuroprotective drugs or treatment strategies to improve the quality of life of stroke patients. Laminaria polysaccharide is an active component that extracts and isolates from

the dried leaves of Laminaria japonica, a plant of the Laminaria family. Its chemical composition includes β-1,3-glycosidic bonds and β-1,6-glycosidic bonds [7]. Studies have shown that Laminaria polysaccharide has a variety of physiological activities such as antioxidant, antilipid, antibacterial, and antitumor, which is of great development value [8]. Studies have reported that laminarin can reduce the development of renal interstitial fibrosis by reducing endoplasmic reticulum stress-mediated apoptosis [9]. Therefore, we speculate that laminarin may also play a corresponding protective role in hypoxic-reperfusion nerve cell injury. Therefore, this study is aimed at exploring the protective effect and potential molecular mechanism of laminarin at different concentrations on OGD/R-induced PC12 nerve cell injury by establishing an OGD/R-induced PC12 nerve cell model.

2. Materials and Methods

2.1. Main Reagents. Laminaria polysaccharide is extracted from kelp. The polysaccharide content was ≥90%. The PC12 cell line was purchased from the Shanghai Institute of cell research, the Chinese Academy of Sciences. DMEM high glucose medium and 10% fetal bovine serum were purchased from GIBCO company of the United States. Penicillin/streptomycin and ROPA cell lysates were from the Invitrogen company of the United States. CCK-8 cell activity test kit and detection kits of tumor necrosis factor-α (TNF-α), interleukin-1β (IL-1β), interleukin-6 (IL-6), reactive oxygen species (ROS), lactate dehydrogenase (LDH), and myeloperoxidase (MPO) were provided by Shanghai Biyuntian Biotechnology Co., Ltd. Annexin V-FITC/PI apoptosis detection kit and BCA protein quantitative detection kit were from the American Becton company. PCNA, Ki67, Bcl-2, Bax, Caspase-3, PTEN, PI3K, p-AKT, GAPDH primary antibody, and HBR-labeled Goat anti-rabbit secondary antibody were purchased from the Beijing Zhongshan Jinqiao company. Other common molecular biology-related antibody reagents and consumables were provided by Thermo Fisher Scientific, USA.

2.2. PC12 Cell Culture and OGD/R Model Construction. PC12 cells were cultured in DMEM high glucose medium containing 10% fetal bovine serum and 1% penicillin/streptomycin. The culture conditions were set at 37°C, 5% CO2 content, and 95% relative humidity. The degree of cell fusion reached more than 90% for subculture. More than three generations of PC12 cells were taken for follow-up experimental research.

The DMEM high glucose medium of logarithmic PC12 cells was first discharged and then washed with PBS for 3 times. A Sugar-free Earle equilibrium salt solution was added to the cells. The cells were then transferred to a 37°C hypoxia incubator (95% N2, 5% CO2, and 1% O2) for 6 hours. Then, the equilibrium solution in the cell culture plate was replaced with DMEM high glucose medium containing 10% fetal bovine serum and placed in a cell culture box at 37°C and 5% CO2 for 24 hours for reoxygenation.

2.3. Experimental Grouping. The extracted Laminaria polysaccharide was diluted into 0.5, 2.5, 5, and 10 μg/ml of serum-free DMEM high glucose culture medium polysaccharide solution. The polysaccharide solution has been ensured to be used in the ultraclean table for sterilization by 0.22 μm pore size filter. According to the experimental requirements, PC12 cells were divided into 5 groups: blank control group (PC12 cells not treated with OGD/R), OGD/R group (PC12 cells treated with OGD/R), OGD/R+laminarin (0.5 μg/ml) group, OGD/R+laminarin (2.5 μg/ml) group, and OGD/R+laminarin (5 μg/ml). The cells in each administration group were incubated for 2 hours before OGD/R modeling.

2.4. Cell Proliferation Activity Was Detected by Cell Counting Kit-8 (CCK-8). PC12 cells in each group were inoculated into 96-well plates at the density of 3×10^3 cells/well. These cells were cultured in a cell incubator at 37°C and 5% CO2 for 24 hours and 20% CO2. Then, 10 μl of CCK-8 solution was added, and cells were continuously incubated for another 2 hours. The microplate reader (Thermo Fisher Scientific, USA) was used to detect the absorbance of PC12 cells at 450 nm.

2.5. Detection of Proinflammatory Factors (TNF-α, IL-1β, and IL-6) and Oxidative Stress Indicators (ROS, LDH, and MPO) by Enzyme-Linked Immunosorbent Assay (ELISA). PC12 cells in each group were inoculated into 96-well plates at the density of 3×10^3 cells/well according to the operating instructions of the ELISA kit. Cells were cultured for 24 hours before collecting the cell supernatant of each group. The expression of TNF-α, IL-1β, IL-6, ROS, LDH, and MPO was examined by ELISA. The absorbance value was measured by a microplate reader.

2.6. Cell Cycle and Apoptosis Were Detected by Flow Cytometry. Cell cycle. PC12 cells in each group were inoculated into 6-well plates at the density of 1×10^6 cells/well and cultured for 48 hours. After culture, the cells were digested with 0.25% trypsin. The cells were then fixed with 70% ethanol at 4°C overnight. Finally, the cells were centrifuged at 1000 r/min for 5 min, and ethanol was discarded. 500 ml PI was added, and cells were incubated in the dark at 37°C for 45 min. The cell cycle was detected by flow cytometry.

Apoptosis. PC12 cells in each group were inoculated into 6-well plates at the density of 1×10^6 cells/well and cultured for 48 hours. After culture, the cells were digested with 0.25% trypsin. The cells were centrifuged at 1000 r/min, and the supernatant was discarded. The cells were resuspended 200 μl combined solution to adjust the cell concentration to 1×10^6 cells/ml. 5 μl PI and 10 μl Annexin V-FITC were added to the suspension. Cells were incubated in the dark for 15 min at room temperature. Apoptosis was detected by flow cytometry.

The FlowJo software (Tree Star, USA) was used to analyze apoptosis and cell-cycle data.

2.7. The Expression Levels of PCNA, Ki67, Bcl-2, Bax, Caspase-3, PTEN, PI3K, and p-AKT Were Detected by Western Blot. The total protein of PC12 cells in each group

was extracted by RIPA cell lysate, and the protein concentration was detected by BCA protein quantitative kit. The extracted total protein was separated by 10% SDS-PAGE and transferred to the PVDF membrane. These membranes were sealed with 5% skimmed milk powder solution for 2 h before mixing with corresponding primary antibody PCNA (ab92552; Abcam), Ki67 (ab16667; Abcam), Bcl-2 (ab32124; Abcam), Bax (ab32503; Abcam), Caspase-3 (cat. No. 9662; Cell Signaling Technology, Inc.), PTEN (ab32199; Abcam), PI3K (ab32089; Abcam), p-AKT (cat. No. 4060; Cell Signaling Technology, Inc.), and GAPDH (ab9485; Abcam). Cells were incubated overnight at 4°C. These membrane proteins were then incubated with HBR-labeled secondary antibodies (cat. No. 7074; Cell Signaling Technology, Inc.) at room temperature for 1 h. ECL chemical kit was used for protein imaging. The value analysis of protein bands was performed through the Image J software. GAPDH was used as the internal reference.

2.8. Statistical Analysis. All data in this experiment were expressed by mean ± standard deviation. All experiments were repeated 3 times, and the data were analyzed with GraphPad prism 7.0. The data difference between the two groups was analyzed by an independent sample t-test. One-way ANOVA analyzed the difference between the three groups and above. $P < 0.05$ was considered to be statistically significant.

3. Results

3.1. Effects of Laminaria Polysaccharide at Different Concentrations on the Viability of PC12 Cells Induced by OGD/R. We first detected the effect of Laminaria polysaccharide at the concentration of 0.5, 2.5, 5, and 10 μg/ml on the viability of PC12 cells. As shown in Figure 1(a), 10 μg/ml laminarin could significantly reduce cell viability compared to the control group ($P < 0.05$). The above results suggest that the concentration of Laminaria polysaccharide around 0.5-5 μg/ml has no toxic effect on the viability of PC12 cells. Therefore, 0.5-5 μg/ml Laminaria polysaccharide was used to construct the subsequent OGD/R model. CCK-8 and Western blot were used to detect the viability of PC12 cells induced by OGD/R. As shown in Figure 1(b), PC12 cell viability in the OGD/R group decreased significantly ($P < 0.05$) than the control group. Laminarin could promote the viability of PC12 cells in a concentration-dependent manner ($P < 0.05$, $P < 0.01$, and $P < 0.001$) compared to the OGD/R group. The recovery of PC12 cell viability was the most obvious at 5 μg/ml Laminaria polysaccharide. As shown in Figure 1(c), the expression of PCNA and Ki67 in the OGD/R group decreased significantly ($P < 0.05$). In addition, the expression levels of PCNA and Ki67 protein in the laminarin group increased gradually with the increase of concentration, and the difference was statistically significant ($P < 0.05$, $P < 0.01$, and $P < 0.001$) than the OGD/R group. The above results showed that Laminaria polysaccharide could play a protective role in alleviating the decline of PC12 cell viability induced by OGD/R.

3.2. Effects of Different Concentrations of Laminaria Polysaccharide on Inflammatory Response and Oxidative Stress Level of PC12 Cells Induced by OGD/R. We then detected the effect of different concentrations of Laminaria polysaccharide on OGD/R-induced proinflammatory factors (TNF- α, IL-1 β, and IL-6) and oxidative stress indicators (ROS, LDH, and MPO) in PC12 cells by ELISA. As shown in Figure 2(a), the expressions of TNF-α, IL-1β, and IL-6 in the OGD/R group were significantly increased ($P < 0.001$) compared with the control group, and laminarin could inhibit TNF-α, IL-1β, and IL-6 ($P < 0.05$, $P < 0.01$, and $P < 0.001$) in a concentration-dependent manner compared with the OGD/R group. In addition, as shown in Figure 2(b), the expressions of ROS, LDH, and MPO in the OGD/R group were significantly increased ($P < 0.001$) compared with the control group, and the levels of ROS, LDH, and MPO in cell supernatant decreased gradually with the increase of laminarin concentration ($P < 0.05$, $P < 0.01$, and $P < 0.001$) compared to the OGD/R group. The above results showed that Laminaria polysaccharide could alleviate the inflammatory response and oxidative stress of PC12 cells induced by OGD/R.

3.3. Effects of Laminaria Polysaccharide at Different Concentrations on PC12 Cell Cycle Induced by OGD/R. The cell cycle was detected by flow cytometry. As shown in Figure 3, the proportion of S-phase cells in the OGD/R group increased significantly than the control group ($P < 0.001$). The proportion of G0/G1 phase cells decreased significantly ($P < 0.05$, $P < 0.01$, and $P < 0.001$), while the proportion of G2/M phase cells did not change significantly. Compared with the OGD/R group, the proportion of S-phase cells decreased significantly ($P < 0.001$), and the proportion of G0/G1 phase cells increased substantially in a concentration-dependent manner ($P < 0.05$, $P < 0.01$, and $P < 0.001$). The above results showed that Laminaria polysaccharide could reduce the S-phase arrest of PC12 cells induced by OGD/R and improve the inhibitory effect of OGD/R on the PC12 cell cycle.

3.4. Effects of Laminaria Polysaccharide at Different Concentrations on Apoptosis of PC12 Cells Induced by OGD/R. Meanwhile, apoptosis was detected by flow cytometry and Western blot. Compared with the control group, the apoptosis rate of the OGD/R group was significantly increased ($P < 0.001$) (Figure 4(a)). Compared with the OGD/R group, laminarin could inhibit apoptosis in a concentration-dependent manner ($P < 0.05$, $P < 0.01$, and $P < 0.001$) (Figure 4(a)). Compared with the control group, the expression levels of apoptotic proteins Bax and Caspase-3 in the OGD/R group were significantly increased ($P < 0.001$), while the expression level of the antiapoptotic protein Bcl-2 was significantly decreased ($P < 0.001$) (Figure 4(b)). With the increase of laminarin concentration, the expression levels of proapoptotic protein Bax and Caspase-3 in PC12 cells gradually decreased, while the expression level of antiapoptotic protein Bcl-2 gradually increased ($P < 0.05$, $P < 0.01$, and $P < 0.001$) (Figure 4(b)).

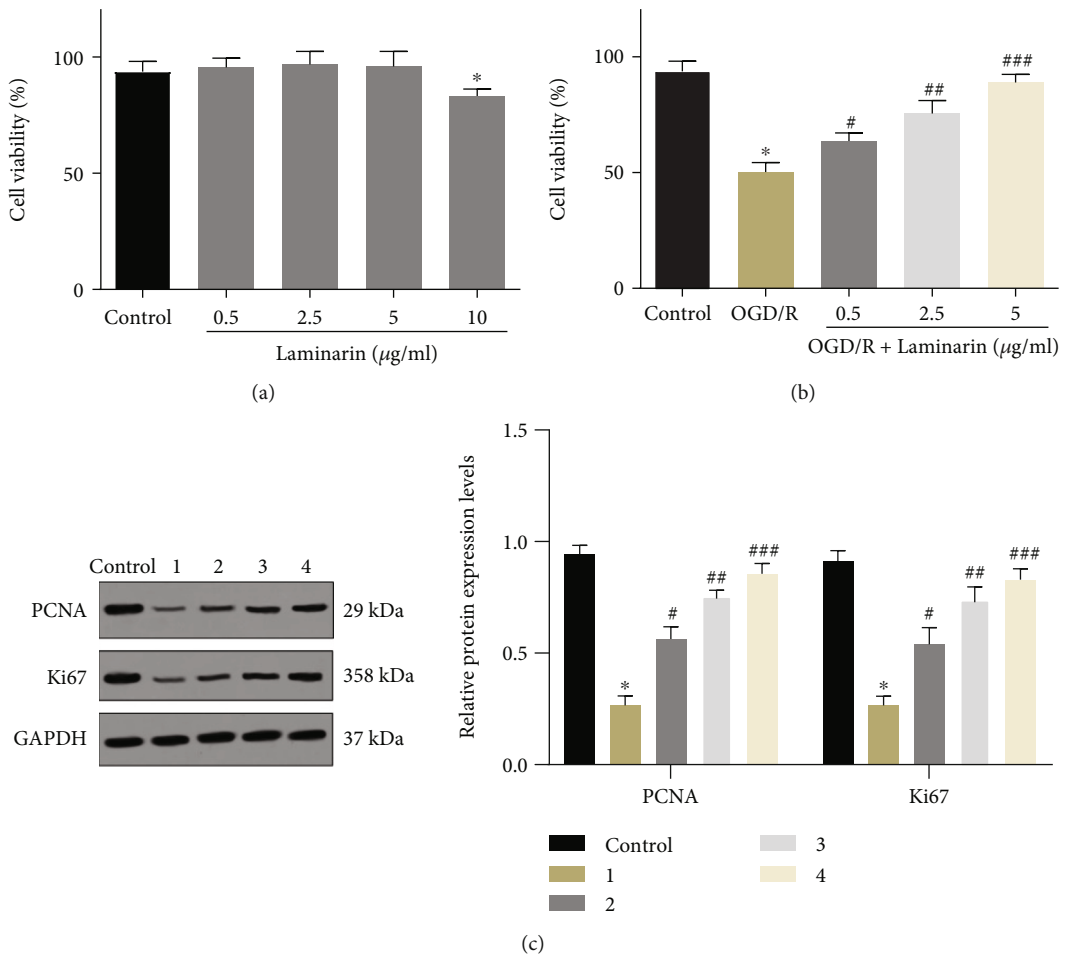

Figure 1: Effect of different concentrations of laminarin on the viability of PC12 cells induced by OGD/R. (a) CCK-8 was used to detect the effects of different concentrations of laminarin (0.5, 2.5, 5, and 10 μg/ml) on the viability of PC12 cells. (b) CCK-8 was conducted to detect the effects of different concentrations of laminarin (0.5, 2.5, and 5 μg/ml) on the viability of PC12 cells induced by OGD/R. (c) Western blot assay was performed to detect the effects of different concentrations of laminarin (0.5, 2.5, and 5 μg/ml) on the protein expression levels of PCNA and Ki67 in PC12 cells induced by OGD/R. Note: 1: OGD/R group, 2: OGD+0.5 μg/ml laminarin group, 3: OGD+2.5 μg/ml laminarin group, and 4: OGD+5 μg/ml laminarin group. Compared with the control group, $^{*}P < 0.05$; compared with the OGD/R group, $^{\#}P < 0.05$, $^{\#\#}P < 0.01$, and $^{\#\#\#}P < 0.001$.

The above results showed that Laminaria polysaccharide could inhibit the apoptosis of PC12 cells induced by OGD/R.

3.5. Effects of Laminaria Polysaccharide at Different Concentrations on the Expression Levels of PTEN, PI3K, and p-AKT Proteins in PC12 Cells Induced by OGD/R. To further study the potential mechanism of Laminaria polysaccharide on OGD/R-induced PC12 cell injury, we detected the expression level of PTEN/PI3K/AKT pathway-related proteins by Western blot. As shown in Figure 5, the protein expressions of PI3K and p-AKT in the OGD/R group were significantly decreased ($P < 0.001$) compared with the control group, while the protein expression of PTEN was significantly increased ($P < 0.001$), and laminarin could upregulate the protein expression of PI3K and p-AKT in a concentration-dependent manner while inhibiting the protein expression of PTEN ($P < 0.05$, $P < 0.01$, and $P < 0.001$). These results suggest that Laminaria polysaccharide can effectively protect PC12 cells from OGD/R-induced injury. Its mechanism may be related to the activation of the PI3K/AKT pathway and the downregulation of PTEN protein.

4. Discussion

At present, the treatment options for ischemic stroke are not satisfactory. Therefore, there is an urgent need to develop new treatment schemes to improve the treatment effect, especially for high-risk patients [10, 11]. This study found that laminarin can reduce OGD/R-induced nerve cell injury by activating PI3K/AKT pathway and downregulating PTEN protein expression. The results indicate that laminarin is a promising candidate drug for treating ischemic stroke, which is worthy of in-depth study.

Due to the characteristics of multitarget and multichannel treatment, studies have confirmed that traditional Chinese medicine significantly promotes the recovery of ischemic stroke [12–15]. For example, in the mouse model of glucose deficiency and hypoxia, tanshinone can effectively

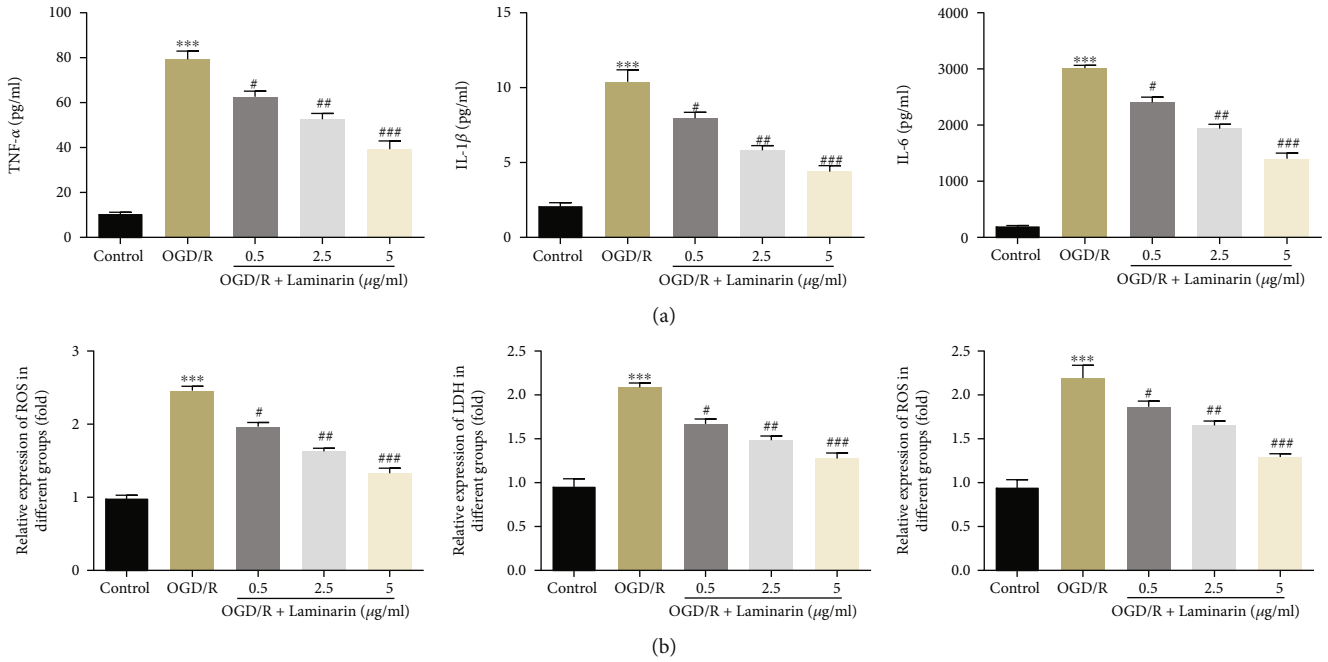

Figure 2: Effect of different concentrations of laminarin on the inflammatory response and oxidative stress of PC12 cells induced by OGD/R. (a) ELISA assay was conducted to detect the effects of different concentrations of laminarin (0.5, 2.5, and 5 μg/ml) on the expression of proinflammatory factors (TNF-α, IL-1β, and IL-6) in PC12 cells induced by OGD/R. (b) ELISA assay was employed to detect the effects of different concentrations of laminarin (0.5, 2.5, and 5 μg/ml) on the expression of oxidative stress-associated factors (ROS, LDH, and MPO) in PC12 cells induced by OGD/R. Note: Compared with the control group, $^{***}P < 0.001$; compared with the OGD/R group, $^{\#}P < 0.05$, $^{\#\#}P < 0.01$, and $^{\#\#\#}P < 0.001$.

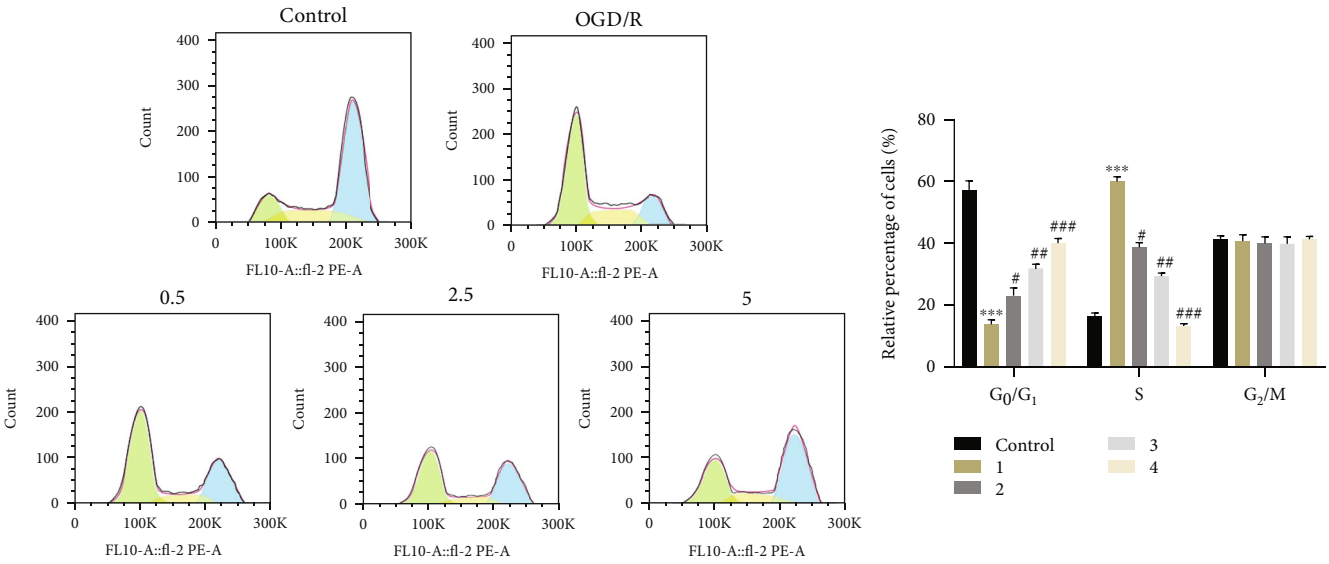

Figure 3: Effect of different concentrations of laminarin (0.5, 2.5, and 5 μg/ml) on the cell-cycle progression of PC12 cells induced by OGD/R. Note: 1: OGD/R group, 2: OGD+0.5 μg/ml laminarin group, 3: OGD+2.5 μg/ml laminarin group, and 4: OGD+5 μg/ml laminarin group. Compared with the control group, $^{***}P < 0.001$; compared with the OGD/R group, $^{\#}P < 0.05$, $^{\#\#}P < 0.01$, and $^{\#\#\#}P < 0.001$.

reduce the area of cerebral infarction in mice [16]. In addition, Ginkgo biloba extract can effectively reduce brain oxygen uptake and consumption in elderly patients with cerebral ischemia to improve the balance between brain oxygen supply and consumption [17]. These studies have confirmed the critical protective effect of traditional Chinese medicine on hypoxic-ischemic brain injury. Laminaria polysaccharide has been widely studied as a kind of macromolecular polysaccharide with many biological functions, including antioxidation and antitumor. However, the role of laminarin in hypoxic-reperfusion nerve injury has not reported. In this study, Laminaria polysaccharide can

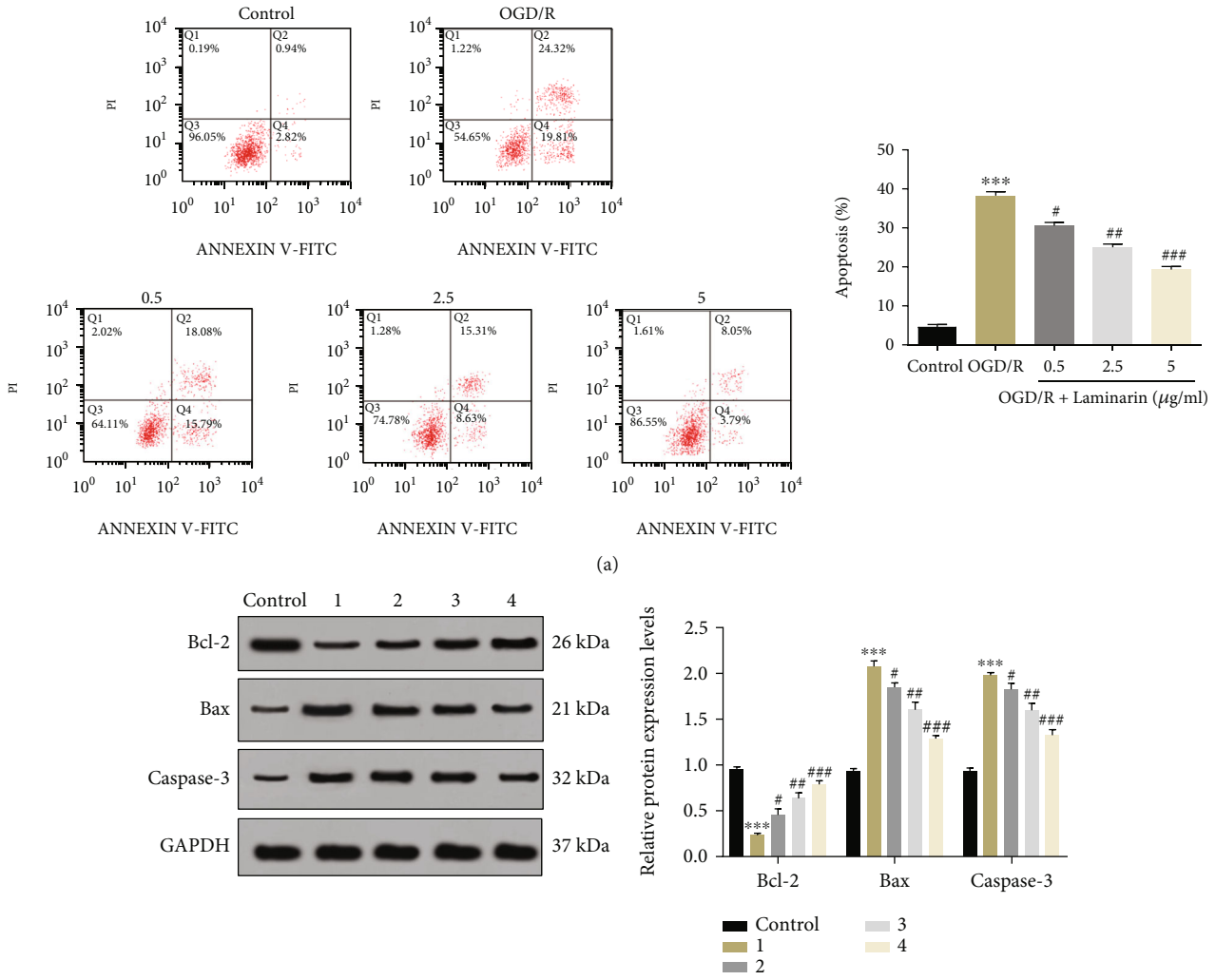

Figure 4: Effect of different concentrations of laminarin (0.5, 2.5, and 5 μg/ml) on the apoptosis of PC12 cells induced by OGD/R. (a) Flow cytometry was used to detect the effects of different concentrations of laminarin (0.5, 2.5, and 5 μg/ml) on apoptosis of PC12 cells induced by OGD/R. (b) Western blot assay was performed to detect the effects of different concentrations of laminarin (0.5, 2.5, and 5 μg/ml) on the protein expression levels of Bcl-2, Bax, and Caspase-3 in PC12 cells induced by OGD/R. Note: 1: OGD/R group, 2: OGD+0.5 μg/ml laminarin group, 3: OGD+2.5 μg/ml laminarin group, and 4: OGD+5 μg/ml laminarin group. Compared with the control group, $^{***}P < 0.001$; compared with the OGD/R group, $^{\#}P < 0.05$, $^{\#\#}P < 0.01$, and $^{\#\#\#}P < 0.001$.

promote the activity of PC12 nerve cells induced by OGD/R in a concentration-dependent manner and reduce the inhibitory effect of OGD/R on the activity of PC12 cells. This result suggests the protective effect of laminarin on ischemia-reperfusion injury.

Cerebral hypoxia reperfusion injury involves multiple pathological processes, including neuroinflammation, oxidative stress, and apoptosis [18–20]. Excessive ROS is widely considered the leading cause of reperfusion injury of microvessels and parenchymal organs in ischemic tissues. After the blood supply of ischemic tissue is restored, excessive free radicals will attack the cells of the tissue and cause damage [21]. At the same time, tissue ischemia can induce proinflammatory cytokines (TNF-α, IL-1β, and IL-6), further aggravating ROS levels [22]. In addition, ischemia-reperfusion injury can also activate cell death programs, including apoptosis, autophagy, and necrosis. There is increasing evidence that excessive proapoptotic proteins (Bax and Caspase-3) and oxidative stress products (LDH and MPO) are produced in cerebral ischemic injury [23, 24]. Previous studies have shown that cinnamon extract transcinnamaldehyde can protect PC12 cells from OGC/R stimulation through antiapoptosis and antioxidant stress [25]. Therefore, targeting inflammation, oxidative stress, and apoptosis has been proved to be a feasible treatment option for cerebral hypoxia reperfusion injury. In this study, we found that OGD/R can induce PC12 neuronal proinflammatory factor (TNF-α, IL-1β, and IL-6) expression and increase the levels of oxidative stress indexes (ROS, LDH, and MPO). At the same time, laminarin could reverse the above effects in a concentration-dependent manner. In addition, the results of flow cytometry showed that laminarin

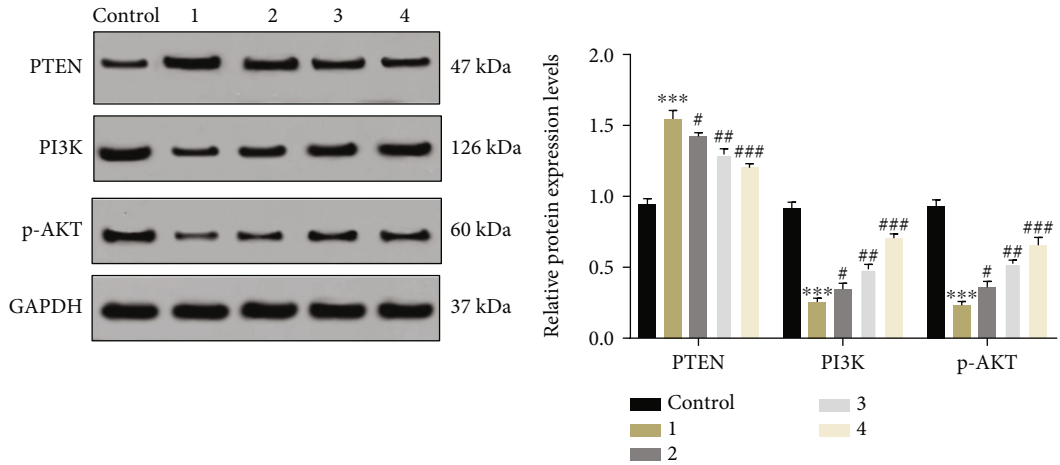

Figure 5: Effects of different concentrations of laminarin (0.5, 2.5, and 5 μg/ml) on the protein expression levels of PTEN, PI3K, and p-AKT in PC12 cells induced by OGD/R. Note: 1: OGD/R group, 2: OGD+0.5 μg/ml laminarin group, 3: OGD+2.5 μg/ml laminarin group, and 4: OGD+5 μg/m. Compared with the control group, $^{***}P < 0.001$; compared with the OGD/R group, $^{\#}P < 0.05$, $^{\#\#}P < 0.01$, and $^{\#\#\#}P < 0.001$.

could alleviate the blocking and proapoptotic effects of OGD/R on the s cycle of PC12 cells. These results suggest that Laminaria polysaccharide can improve ischemia-reperfusion nerve cell injury by regulating inflammatory factors, oxidative stress-related indexes, and cycle-related proteins.

Finally, we studied the possible molecular mechanism of laminarin in protecting nerve cells from ischemia-reperfusion injury. PTEN is a tumor suppressor gene with bispecific phosphatase activity, mainly responsible for regulating cell growth and apoptosis signal transduction [26]. Many studies have shown that PTEN gene knockout can protect against ischemia-reperfusion nerve injury [27]. For example, SETD5-AS1 can increase cerebral infarction volume and neurological impairment in ischemic stroke mice by inducing PTEN overexpression [28]. Andrographolide of traditional Chinese medicine can protect hippocampal neurons in rats with chronic cerebral ischemia injury by inhibiting PTEN levels [29]. In addition, PI3K/AKT is a vital pathway closely related to apoptosis after cerebral hypoxia and ischemia. PTEN can promote cell activity damage by antagonizing PI3K/AKT pathway to induce cell-cycle arrest [30]. Studies have shown that Panax notoginseng saponins improve hypoxic-ischemic neonatal brain injury by activating the PI3K/AKT pathway [31]. Curcumin can target vascular endothelial growth factors by activating PI3K/AKT to prevent cerebral hypoxic-ischemic injury in neonatal rats [32]. In this study, Laminaria polysaccharide can effectively inhibit the PTEN level of PC12 cells induced by OGD/R and promote the levels of PI3K and p-AKT, suggesting that Laminaria polysaccharide can reduce nerve cell injury after ischemia-reperfusion by regulating PTEN/PI3K/AKT pathway.

In conclusion, laminarin can inhibit OGD/R-induced inflammation, oxidative stress, and apoptosis of PC12 cells by regulating PTEN/PI3K/AKT pathway. These results provide new insights into the protective mechanism of laminarin against cerebral hypoxia and ischemia and indicate that laminarin is a promising choice for treating ischemic stroke. However, this study has not verified the effect of Laminaria polysaccharide on brain injury in hypoxic mice, which will be further studied in a follow-up study.

Data Availability

The data used to support the findings of this study are included within the article.

Conflicts of Interest

The authors have no conflicts of interest to declare.

Acknowledgments

This research was supported by the Weifang Medical Sciences Research Project (No. 2020YX058).

References

[1] J. Kim, T. Thayabaranathan, G. A. Donnan et al., "Global stroke statistics 2019," *International Journal of Stroke*, vol. 15, no. 8, pp. 819–838, 2020.

[2] A. Nitzsche, M. Poittevin, A. Benarab et al., "Endothelial S1P1 signaling counteracts infarct expansion in ischemic stroke," *Circulation Research*, vol. 128, no. 3, pp. 363–382, 2021.

[3] W. J. Tu, X. W. Zeng, A. Deng et al., "Circulating FABP4 (fatty acid–binding protein 4) is a novel prognostic biomarker in patients with acute ischemic stroke," *Stroke*, vol. 48, no. 6, pp. 1531–1538, 2017.

[4] A. Brassai, R. G. Suvanjeiev, E. G. Bán, and M. Lakatos, "Role of synaptic and nonsynaptic glutamate receptors in ischaemia induced neurotoxicity," *Brain Research Bulletin*, vol. 112, pp. 1–6, 2015.

[5] O. Maier, B. H. Menze, J. von der Gablentz et al., "ISLES 2015-a public evaluation benchmark for ischemic stroke lesion segmentation from multispectral MRI," *Medical Image Analysis*, vol. 35, pp. 250–269, 2017.

[6] J. Zhao, Y. Bai, C. Zhang et al., "Cinepazide maleate protects PC12 cells against oxygen–glucose deprivation-induced injury," *Neurological Sciences*, vol. 35, no. 6, pp. 875–881, 2014.

[7] L. Y. Xiu, "Research progress of laminarin. Journal of Anhui," *Agricultural Sciences*, vol. 27, 2010.

[8] M. Zargarzadeh, A. J. R. Amaral, C. A. Custódio, and J. F. Mano, "Biomedical applications of laminarin," *Carbohydrate Polymers*, vol. 15, no. 232, article 115774, 2020.

[9] C. Zhang, J. Gao, and L. Zhang, "Effect of laminarin on the expression of GRP78 and GRP94 in rat after unilateral ureteral obstruction," *Scandinavian Journal of Urology and Nephrology*, vol. 46, no. 4, pp. 267–272, 2012.

[10] F. Herpich and F. Rincon, "Management of acute ischemic stroke," *Critical Care Medicine*, vol. 48, no. 11, pp. 1654–1663, 2020.

[11] D. Kuriakose and Z. Xiao, "Pathophysiology and treatment of stroke: present status and future perspectives," *International Journal of Molecular Sciences*, vol. 21, no. 20, p. 7609, 2020.

[12] T. Liu, Y. Ding, and A. Wen, "Traditional Chinese medicine for ischaemic stroke," *Lancet Neurology*, vol. 17, no. 9, p. 745, 2018.

[13] S. C. Donnelly, "Traditional Chinese medicine treatment post-stroke and a significant reduction in presentation to healthcare providers," *QJM*, vol. 112, no. 6, p. 397, 2019.

[14] Y. Yuwen, N.-n. Shi, X.-j. Han et al., "Appraisal of clinical practice guidelines for ischemic stroke management in Chinese medicine with appraisal of guidelines for research and evaluation instrument: a systematic review," *Chinese Journal of Integrative Medicine*, vol. 21, no. 9, pp. 707–715, 2015.

[15] W. S. Chen, H. C. Hsu, Y. W. Chuang et al., "Predictors for the use of traditional Chinese medicine among inpatients with first-time stroke: a population-based study," *BMC Complementary Medicine and Therapies*, vol. 20, no. 1, p. 244, 2020.

[16] J. C. Lee, J. H. Park, O. K. Park et al., "Neuroprotective effects of tanshinone I from Danshen extract in a mouse model of hypoxia-ischemia," *Anatomy & cell biology*, vol. 46, no. 3, pp. 183–190, 2013.

[17] L. Xu, Z. Hu, J. Shen, and P. M. McQuillan, "Effects of _Ginkgo biloba_ extract on cerebral oxygen and glucose metabolism in elderly patients with pre-existing cerebral ischemia," *Complementary Therapies in Medicine*, vol. 23, no. 2, pp. 220–225, 2015.

[18] T. H. Sanderson, C. A. Reynolds, R. Kumar, K. Przyklenk, and M. Hüttemann, "Molecular mechanisms of ischemia–reperfusion injury in brain: pivotal role of the mitochondrial membrane potential in reactive oxygen species generation," *Molecular Neurobiology*, vol. 47, no. 1, pp. 9–23, 2013.

[19] L. Gong, Y. Tang, R. An, M. Lin, L. Chen, and J. du, "RTN1-C mediates cerebral ischemia/reperfusion injury via ER stress and mitochondria-associated apoptosis pathways," *Cell Death & Disease*, vol. 8, no. 10, article e3080, 2017.

[20] D. D. Zhang, M. J. Zou, Y. T. Zhang et al., "A novel IL-1RA-PEP fusion protein with enhanced brain penetration ameliorates cerebral ischemia-reperfusion injury by inhibition of oxidative stress and neuroinflammation," *Experimental Neurology*, vol. 297, pp. 1–13, 2017.

[21] D. A. Parks and D. N. Granger, "Ischemia-reperfusion injury: a radical view," *Hepatology*, vol. 8, no. 3, pp. 680–682, 1988.

[22] H. K. Eltzschig and T. Eckle, "Ischemia and reperfusion-from mechanism to translation," *Nature Medicine*, vol. 17, no. 11, pp. 1391–1401, 2011.

[23] A. Majid, "Neuroprotection in stroke: past, present, and future," *International Scholarly Research Notices*, vol. 2014, Article ID 515716, 17 pages, 2014.

[24] H. Wu, C. Tang, L. W. Tai et al., "Flurbiprofen axetil attenuates cerebral ischemia/reperfusion injury by reducing inflammation in a rat model of transient global cerebral ischemia/reperfusion," *Bioscience Reports*, vol. 38, no. 4, 2018.

[25] X. Qi, R. Zhou, Y. Liu et al., "Trans-cinnamaldehyde protected PC12 cells against oxygen and glucose deprivation/reperfusion (OGD/R)-induced injury via anti-apoptosis and anti-oxidative stress," *Molecular and Cellular Biochemistry*, vol. 421, no. 1-2, pp. 67–74, 2016.

[26] A. Papa and P. P. Pandolfi, "The PTEN-PI3K axis in cancer," *Biomolecules*, vol. 9, no. 4, p. 153, 2019.

[27] M. Y. Diao, Y. Zhu, J. Yang et al., "Hypothermia protects neurons against ischemia/reperfusion-induced pyroptosis via m6A-mediated activation of PTEN and the PI3K/Akt/GSK-3β signaling pathway," *Brain Research Bulletin*, vol. 159, pp. 25–31, 2020.

[28] S. Y. Miao, S. M. Miao, R. T. Cui, A. L. Yu, and Z. J. Miao, "SETD5-AS1 stimulates neuron death in stroke via promoting PTEN expression," *European Review for Medical and Pharmacological Sciences*, vol. 22, no. 18, pp. 6035–6041, 2018.

[29] D. P. Wang, S. H. Chen, D. Wang et al., "Neuroprotective effects of andrographolide on chronic cerebral hypoperfusion-induced hippocampal neuronal damage in rats possibly via PTEN/AKT signaling pathway," *Acta Histochemica*, vol. 122, no. 3, article 151514, 2020.

[30] N. Nakamura, S. Ramaswamy, F. Vazquez, S. Signoretti, M. Loda, and W. R. Sellers, "Forkhead transcription factors are critical effectors of cell death and cell cycle arrest downstream of PTEN," *Molecular and Cellular Biology*, vol. 20, no. 23, pp. 8969–8982, 2000.

[31] L. Tu, Y. Wang, D. Chen et al., "Protective effects of notoginsenoside r1 via regulation of the PI3K-Akt-mTOR/JNK pathway in neonatal cerebral hypoxic–ischemic brain injury," *Neurochemical Research*, vol. 43, no. 6, pp. 1210–1226, 2018.

[32] J. Li, Y. An, J. N. Wang, X. P. Yin, H. Zhou, and Y. S. Wang, "Curcumin targets vascular endothelial growth factorviaactivating the PI3K/Akt signaling pathway and improves brain hypoxic-ischemic injury in neonatal rats," *The Korean Journal of Physiology & Pharmacology*, vol. 24, no. 5, pp. 423–431, 2020.

Hindawi
Advances in Polymer Technology
Volume 2022, Article ID 6934934, 6 pages
https://doi.org/10.1155/2022/6934934

Research Article

Administration of Iodine-125 Seeds Promotes Apoptosis in Cholangiocarcinoma through the PI3K/Akt Pathway

Junqing Lin, Leye Yan, Xiaolong Wang, Zhengzhong Wu, Kun Ke, Xin Lin, Ning Huang, and Weizhu Yang

Department of Interventional Radiology, Fujian Medical University Union Hospital, Fuzhou 350001, China

Correspondence should be addressed to Weizhu Yang; drweizhuyang@163.com

Received 30 December 2021; Accepted 26 January 2022; Published 24 February 2022

Academic Editor: Changlei Xia

Purpose. We aimed to examine the effects of ^{125}I seeds on the gene expression of Bcl-2, Bax, and PI3K/Akt pathway components in cholangiocarcinoma cells. *Methods*. In vitro, human cholangiocarcinoma RBE cells were treated with ^{125}I seeds (0.39 mCi or 0.85 mCi) for 72 h, 120 h, and 168 h. Cell proliferation and apoptosis were assessed. The expression of Bcl-2 and Bax was detected by RT-PCR, and Western blotting was carried out to explore changes in Akt activity. *Result*. ^{125}I seeds inhibited the proliferation of RBE cells. The apoptosis rate of the RBE cells in the low-activity group was significantly higher than that in the high-activity group at 120 h and 168 h, while no difference was found between the two groups at 72 h. After 120 h of culture, the gene expression of Bcl-2 and Bax decreased in both groups, the ratio of Bcl − 2/Bax in the low-activity group decreased, and the PI3K/Akt signaling pathway was inhibited in both groups. *Conclusion*. ^{125}I seeds affect the proliferation and apoptosis of cholangiocarcinoma cells in a dose-dependent manner. The therapeutic effect of low-activity ^{125}I seeds on cancer cells may be better. ^{125}I seed brachytherapy may promote the apoptosis of cholangiocarcinoma cells by inhibiting the PI3K/Akt signaling pathway and regulating the Bcl − 2/Bax ratio.

1. Introduction

Cholangiocarcinoma (CCA) is the second most common malignant liver carcinoma, accounting for 3% of gastrointestinal cancer cases and 15% of all primary hepatic tumor cases [1, 2]. The incidence and mortality of CCA have been steadily increasing in recent decades, especially in Asian countries [3, 4]. CCA is a highly aggressive tumor that is associated with a high mortality rate due to late diagnosis and infective treatment [5]. Early-stage CCA can be treated by surgical resection alone or in combination with liver transplantation. However, at the time of diagnosis, the majority of patients (>65%-80%) are in an advanced stage of disease, with unresectable or distant metastasis, and no effective chemotherapies or molecular targeted therapies are available for these patients [6]. Therefore, there is an urgent need to develop new therapeutic strategies for CCA.

^{125}I seed brachytherapy is an established approach for the treatment of a variety of tumors, such as hepatocellular carcinoma, prostate cancer, lung cancer, and pulmonary cancer, and has resulted in excellent outcomes. ^{125}I seed brachytherapy has been demonstrated to be an effective modality with advantages of maximal antitumor effects, minimal toxicity and morbidity, slow and continuous irradiation release, convenience, short hospital stay, and long-term efficacy [7, 8]. To date, ^{125}I seed implantation alone or in combination with biliary stents has been used in CCA patients to evaluate the benefits.

Apoptosis, DNA damage, G2/M phase cell cycle arrest, autophagy, and paraptosis are possible mechanisms underlying the effect of ^{125}I seed radiation on various types of cancer [9–11]. Apoptotic programmed cell death plays a key role in a number of human physiological and pathological processes via the extrinsic (death receptor) and intrinsic (mitochon-

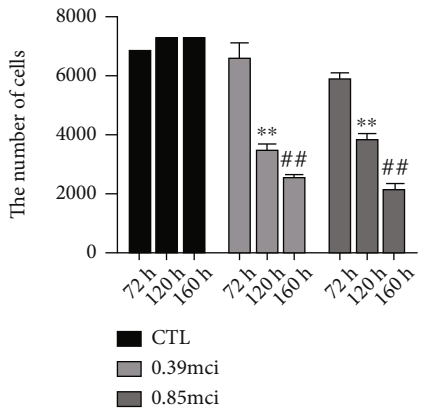

FIGURE 1: Proliferation analysis of the RBE cells treated with low-activity (0.39 mCi), high-activity (0.85 mCi), and control groups at 72 h, 120 h, and 168 h. Significant difference was detected between the low-activity and control groups ($^{**}P < 0.001$), as well as the high-activity and control groups ($^{\#\#}P < 0.00$).

drial) pathways [12–14]. Mitochondrial apoptosis is tightly controlled by BCL-2 family proteins, including apoptosis-inhibiting molecules (such as Bcl-2) and apoptosis-promoting molecules (such as Bax) [15].

The phosphatidylinositol 3′-kinase (PI3K)/Akt pathway is a key regulator of cellular functions, including proliferation, migration, invasion, and survival, and appears to be crucial in cancer [16]. Akt regulates a variety of biological processes, including the inhibition of apoptosis, which is mediated by the direct phosphorylation of apoptotic signaling molecules or the indirect modulation of transcription factor activity [17]. Moreover, through inactivating the original prosurvival Bcl-2 family members, Akt negatively regulates the expression or function of Bcl-2 homology domain 3-only proteins [18]. Therefore, in the present study, we investigated whether ^{125}I seeds can be exploited as a novel effective strategy for treating CCA via the regulation of BCL-2 family proteins by PI3K signaling.

2. Methods and Materials

2.1. Cell Culture. Human cholangiocarcinoma RBE cells were provided by the Cell Bank of Type Culture Collection of the Chinese Academy of Sciences (Shanghai, China). RBE cells were cultured in RPMI 1640 culture medium (Gibco, Carlsbad, CA) supplemented with 10% fetal bovine serum and 1% penicillin-streptomycin in a humidified incubator containing 5% CO_2 at 37°C. The media were replaced every other day. When the cells formed a 70%-80% confluent monolayer, they were detached with 0.25% trypsin-EDTA and dissociated into a single-cell suspension for further cell culture and assays.

2.2. Radiation Source. The ^{125}I seeds used during the study period were kindly provided by Jaco Pharmaceuticals Company Limited (Ningbo, China). The ^{125}I seeds had a half-life of 59.4 days, were 4.5 mm in length and 0.8 mm in diameter, and were sterilized by high-temperature sterilization. Cells were cultured at a density of 2000 cells/well in 96-well plates. After overnight culture, one sterilized ^{125}I seed was placed in the center of each of 6 wells, and these wells were divided into the low-activity (0.39 mCi/seed), high-activity (0.85 mCi/seed), and control treatment groups.

2.3. Cell Apoptosis Assay. After ^{125}I seed treatment, Hoechst/PI double staining was performed, and cell apoptosis was assessed through high-content screening. Cells were cultured at a density of 2000 cells/well in 96-well plates and treated with low-activity ^{125}I seeds, high-activity ^{125}I seeds, or no ^{125}I seeds in the center of each of 6 wells. Each sample was analyzed at 72 h, 120 h, and 168 h. The apoptosis rate was expressed as the percentage of the highest target total intensity.

2.4. Real-Time PCR Analysis. RBE cells were collected 120 h after irradiation, and ribonucleic acid (RNA) was isolated from the cultured cells. Total RNA was extracted by Biozol (BioFlux, Japan), and reverse transcription was performed with a PrimeScript RT Kit (Takara Bio Inc., Japan) according to the manufacturer's protocol. The synthesized cDNA was quantified with a LightCycler 96 Real-Time PCR system (Roche, UK) and SYBR Premix Ex Taq (Tli RNaseH Plus) (Takara Bio Inc., Japan). The specificity of the primers was verified by analyzing the melting curve. The expression level was standardized by the internal reference gene GAPDH, and the relative expression was determined by the $2^{-\Delta\Delta Ct}$ method. Quantitative real-time PCR was used to assess the relative Bcl-2 and Bax gene expression levels.

2.5. Western Blotting Analysis. Cell lysates were obtained after treatment with high- or low-activity seeds for 120 h, subjected to SDS-polyacrylamide gel electrophoresis, and immunoblotted with primary antibodies (rabbit monoclonal anti-phospho-Akt; Ser473: Cell Signaling Technology, USA), followed by horseradish peroxidase-conjugated secondary antibodies. The bands were visualized by enhanced chemiluminescence (ECL, Thermo Scientific Pierce, USA) using a lumino image analyzer. The images were processed and analyzed by the ImageJ software.

2.6. Statistical Analysis. All the data are expressed as the mean ± standard deviation ($x \pm s$). A t test was used to compare the mean values of two groups. The statistical significance of mean differences between studied groups was evaluated by two-way ANOVA and Dunnett's test. Statistical significance was defined as a P value < 0.05. Statistical calculations were performed with the SPSS 13.0 software.

3. Results

3.1. Proliferation Analysis. RBE cells were treated with ^{125}I seeds of different activities, and the proliferation of the RBE cells was detected by a high-content screening instrument at 72 h, 120 h, and 168 h. There was no significant difference in cell proliferation between the high-activity group and the low-activity group after 72 hours of incubation, but significant differences were detected at 120 hours and 168 hours. With the increase in treatment time, the number of proliferating cells decreased significantly, and there was a

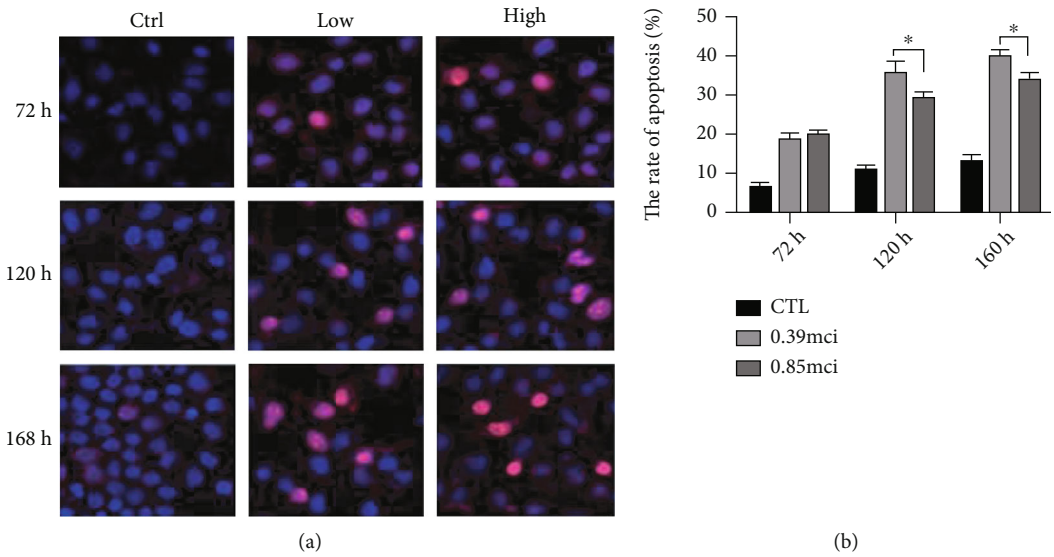

Figure 2: Apoptosis analysis of the RBE cells treated with low-activity (0.39 mCi), high-activity (0.85 mCi), and control groups at 72 h, 120 h, and 168 h. (a) Hoechst/PI double staining and (b) cell apoptosis rate was performed through high-content screening ($^{*}P < 0.05$).

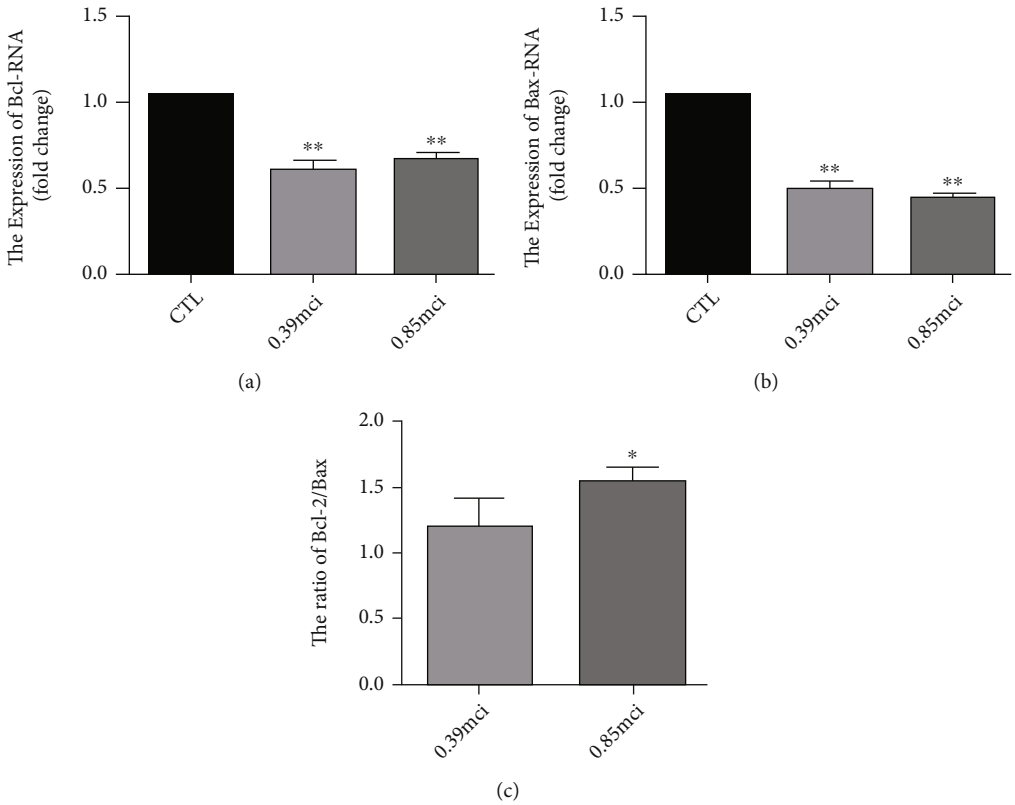

Figure 3: Bcl-2 and Bax gene expression levels in the control group, low-activity group, and high-activity group by RT-PCR. (a) RNA levels of Bcl-2. (b) RNA levels of Bax. (c) The ratio of Bcl − 2/Bax ($^{*}P < 0.05$, $^{**}P < 0.001$).

significant difference within each group except for the control group, while there was no significant difference between the high-activity group and the low-activity group. The rate of cell proliferation inhibition increased with time (Figure 1).

3.2. Apoptosis Analysis. The apoptosis rates of the RBE cells treated with low-activity and high-activity ^{125}I seeds were significantly higher than that of the RBE cells treated with control after 72 h, 120 h, and 168 h of treatment. At 72 h, the apoptosis rate of RBE cells in the low-activity group

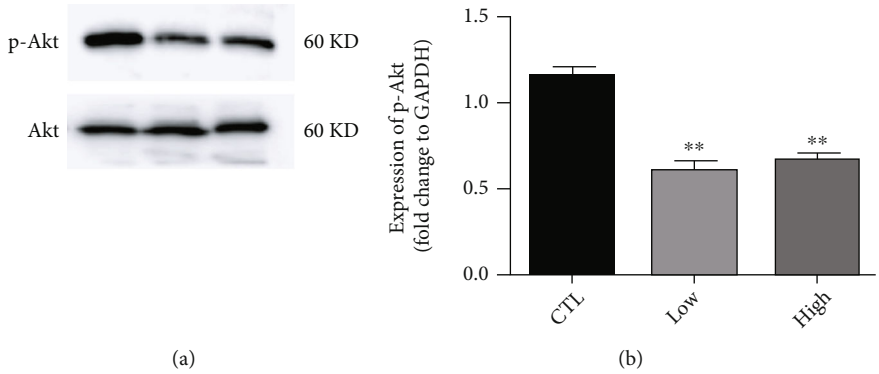

Figure 4: Expression of p-Akt in the cells treated with high- and low-activity ^{125}I seeds for 120 h. (a) Western blotting analysis of expression of p-Akt. (b) Histograms relative to the quantification of the marker bands in (a) ($^{**}P < 0.001$).

(0.39 mCi) was not significantly different from that in the high-activity group (0.85 mCi), but at 120 h and 168 h, the difference was statistically significant ($P < 0.05$) (Figure 2).

3.3. Bcl-2 and Bax Gene Expression Levels. After the cells were treated with high- and low-activity ^{125}I seeds for 120 hours, the levels of Bcl-2 and Bax RNA expression were detected in the control group, low-activity group, and high-activity group. The expression of Bcl-2 and Bax was decreased in both the low- and high-activity groups. The expression of Bcl-2 in the low-activity group was lower than that in the high-activity group, while the expression of Bax in the low-activity group was higher than that in the high-activity group. The ratio of Bcl − 2/Bax was 1.20 in the low-activity group and 1.56 in the high-activity group (Figure 3).

3.4. PI3K/Akt Signaling Pathway. Western blotting was used to detect the expression of p-Akt in the cells treated with high- and low-activity ^{125}I seeds for 120 h. The level of p-Akt in the low- and high-activity groups was significantly lower than that in the control group. However, there was no significant difference in the level of phosphorylated Akt between the low-activity and high-activity groups (Figure 4).

4. Discussion

CCA is a rare cancer that constitutes a diverse group of malignancies emerging from the biliary tree [19, 20]. However, CCA has been a global health problem, and its global incidence and mortality have increased in recent decades. CCA is often asymptomatic at an early stage and diagnosed at an advanced stage, resulting in a poor prognosis. Thus, novel therapeutic strategies need to be developed. ^{125}I seed implantation alone or in combination with biliary stents has been used in CCA patients, indicating that ^{125}I seed treatment is an effective adjuvant therapy [21–23].

Previous studies have reported that irradiation-induced apoptosis became more obvious when the radiation dose increased [24], which is similar to the results of the present study. In our study, we found that cell proliferation was not significantly affected in either the low-activity group or the high-activity group after 72 hours of treatment. At 120 hours and 168 hours, the proliferation of cells in the low-activity group and high-activity group was significantly inhibited, and it increased with time. It is suggested that the inhibitory effects of ^{125}I seeds on tumor cells are dose-dependent. Moreover, there was no significant difference in the apoptosis rate at 72 hours. However, at 120 hours and 168 hours, the apoptosis rate of the low-activity group was higher than that of the high-activity group, which was consistent with other studies [25]. Therefore, a lower dose was also more effective in inducing apoptosis in cancer cells. It is worth noting that the effect of promoting tumor cell apoptosis in the low-activity group was better than that in the high-activity group, which may be related to the reactive protection of cells after injury.

The Bcl-2 family plays a pivotal role in apoptosis progression and can activate cell death by activating the mitochondrial pathway. The Bcl-2 family can be divided into three groups: prosurvival BCL-2-like proteins, multi-BH domain proapoptotic BAX/BAK proteins, and proapoptotic BH3-only proteins [26]. Bcl-2 family genes are also involved in the imbalance of cell growth and death in some cancers, which may be related to BH3 domain mutations in proapoptotic and antiapoptotic proteins. Overexpression of members of the BCL-2 protein family that block apoptosis contributes to malignant transformation [27]. There is potential evidence that inhibition of Bcl-2-like protein expression can be a therapeutic strategy for cancer. Several studies revealed that ^{125}I seed radiation could significantly upregulate the expression of Bax protein and downregulate the expression of Bcl-2 protein in lung cancer cells [25, 28]. Consistent with the above reports, current results supported that ^{125}I seed brachytherapy upregulates Bax RNA expression and downregulates Bcl-2 RNA expression, especially in the low-activity group. Furthermore, the ratio of Bcl − 2/Bax in the low-activity group was lower than that in the high-activity group, which indicated that the treatment effect in the low-activity group is better than that in the high-activity group.

Moreover, the PI3K/Akt signaling pathway plays a vital role in cellular processes, including cell proliferation, differentiation, and migration, apoptosis, and autophagy, as well as in maintaining many basic physiological functions, such as nutrient absorption, ribosome synthesis, and intracellular metabolism. Akt mainly includes three isoforms, AKT1,

AKT2, and AKT3, that share a common structure and a similar activation mechanism [29]. All three subtypes have highly conserved domains at the N-terminus. After activation by phosphorylation of Thr308 or Ser473, Akt is transferred into the cytoplasm or nucleus, phosphorylates a variety of downstream protein substrates, and regulates various cell processes, including metabolism, proliferation, survival, transcription, and angiogenesis. Akt also affects Bcl-2 family proteins, which play a regulatory role in metabolism, survival, and proliferation. Akt activates the antiapoptotic role of Bcl-2 and Bcl-xL by facilitating the interaction between phosphorylated BAD and 14-3-3 protein and inhibiting the activity of caspase-9. Furthermore, activated AKT translocates to various intracellular locations and phosphorylates and modulates the function of numerous substrates that are involved in cancer initiation and progression [29]. Several studies have suggested that the AKT signaling pathway plays an essential role in ^{125}I seeds-based radiotherapy of cancer cells [9, 10, 30–32]. In our study, the level of phosphorylation of PI3K/Akt pathway components was detected to assess the activation of the PI3K/Akt pathway. The phosphorylation of Akt in the low-activity group and high-activity group was lower than that in the control group, but there was no significant difference in the level of pathway activation between these two groups. Radiation from ^{125}I seeds downregulated the expression of p-Akt, and ^{125}I seed radiation-induced apoptosis in CCA may be caused by the inhibition of activation of Akt signaling.

There are some limitations in this study. First, the ^{125}I seed irradiation scheme designed in this experiment has the disadvantage of uneven irradiation. Then, the cumulative dose received using only one ^{125}I seed could not be calculated from the corresponding activity of the treatment in this study. Further in vivo studies need to be performed to verify the results of this in vitro experiment.

5. Conclusion

^{125}I seeds affect the proliferation and apoptosis of cholangiocarcinoma cell lines. The therapeutic effect of low-activity ^{125}I seeds on cancer cells may be better than that of high-dose ^{125}I seeds. ^{125}I seed therapy may affect the balance of Bcl − 2/Bax by regulating the activity of the PI3K/Akt signaling pathway.

Data Availability

The data used to support the findings of this study are included within the article.

Conflicts of Interest

The authors report no conflict of interest.

Acknowledgments

This work is sponsored by grants from the Fujian Provincial Department of Science and Technology (2019J01162).

References

[1] J. M. Banales, J. J. G. Marin, A. Lamarca et al., "Cholangiocarcinoma 2020: the next horizon in mechanisms and management," *Nature Reviews. Gastroenterology & Hepatology*, vol. 17, no. 9, pp. 557–588, 2020.

[2] I. Ntanasis-Stathopoulos, D. I. Tsilimigras, M. Gavriatopoulou, D. Schizas, and T. M. Pawlik, "Cholangiocarcinoma: investigations into pathway-targeted therapies," *Expert Review of Anticancer Therapy*, vol. 20, no. 9, pp. 765–773, 2020.

[3] C. J. O'Rourke, J. Lafuente-Barquero, and J. B. Andersen, "Epigenome remodeling in cholangiocarcinoma," *Trends in Cancer*, vol. 5, no. 6, pp. 335–350, 2019.

[4] P. M. Rodrigues, P. Olaizola, N. A. Paiva et al., "Pathogenesis of cholangiocarcinoma," *Annual Review of Pathology*, vol. 16, no. 1, pp. 433–463, 2021.

[5] P. Bertuccio, M. Malvezzi, G. Carioli et al., "Global trends in mortality from intrahepatic and extrahepatic cholangiocarcinoma," *Journal of Hepatology*, vol. 71, no. 1, pp. 104–114, 2019.

[6] D. Dondossola, M. Ghidini, F. Grossi, G. Rossi, and D. Foschi, "Practical review for diagnosis and clinical management of perihilar cholangiocarcinoma," *World Journal of Gastroenterology*, vol. 26, no. 25, pp. 3542–3561, 2020.

[7] F. Li, L. Wang, Y. Zhang et al., "A retrospective study on using a novel single needle cone puncture approach for the iodine-125 seed brachytherapy in treating patients with thoracic malignancy," *Frontiers in Oncology*, vol. 11, article 640131, 2021.

[8] J. Lin, H. Jiang, W. Yang et al., "Predictive factors of benefit from iodine-125 brachytherapy for hepatocellular carcinoma with portal vein tumor thrombosis," *Brachytherapy*, vol. 18, no. 2, pp. 233–239, 2019.

[9] L. Hu, H. Wang, Y. Zhao, and J. Wang, "125I seeds radiation induces paraptosis-like cell death via PI3K/AKT signaling pathway in HCT116 cells," *BioMed Research International*, vol. 2016, Article ID 8145495, 2016.

[10] C. Wang, T. K. Li, C. H. Zeng et al., "Iodine125 seed radiation induces ROS mediated apoptosis, autophagy and paraptosis in human esophageal squamous cell carcinoma cells," *Oncology Reports*, vol. 43, no. 6, pp. 2028–2044, 2020.

[11] J. Lin, W. Yang, N. Jiang et al., "Incidence and prediction of seed migration to the chest after iodine-125 brachytherapy for hepatocellular carcinoma," *Brachytherapy*, vol. 16, no. 6, pp. 1252–1256, 2017.

[12] R. A. Lockshin, "Programmed cell death 50 (and beyond)," *Cell Death and Differentiation*, vol. 23, no. 1, pp. 10–17, 2016.

[13] H. Flores-Romero, O. Landeta, B. Ugarte-Uribe et al., "BFL1 modulates apoptosis at the membrane level through a bifunctional and multimodal mechanism showing key differences with BCLXL," *Cell Death and Differentiation*, vol. 26, no. 10, pp. 1880–1894, 2019.

[14] C. Boedicker, M. Hussong, C. Grimm et al., "Co-inhibition of BET proteins and PI3Kα triggers mitochondrial apoptosis in rhabdomyosarcoma cells," *Oncogene*, vol. 39, no. 19, pp. 3837–3852, 2020.

[15] T. P. Garner, D. Amgalan, D. E. Reyna, S. Li, R. N. Kitsis, and E. Gavathiotis, "Small-molecule allosteric inhibitors of BAX," *Nature Chemical Biology*, vol. 15, no. 4, pp. 322–330, 2019.

[16] C. Porta, C. Paglino, and A. Mosca, "Targeting PI3K/Akt/mTOR signaling in cancer," *Frontiers in Oncology*, vol. 4, p. 64, 2014.

[17] A. Bender, D. Opel, I. Naumann et al., "PI3K inhibitors prime neuroblastoma cells for chemotherapy by shifting the balance towards pro-apoptotic Bcl-2 proteins and enhanced mitochondrial apoptosis," *Oncogene*, vol. 30, no. 4, pp. 494–503, 2011.

[18] Y. He, M. M. Sun, G. G. Zhang et al., "Targeting PI3K/Akt signal transduction for cancer therapy," *Signal Transduction and Targeted Therapy*, vol. 6, no. 1, p. 425, 2021.

[19] J. M. Banales, V. Cardinale, G. Carpino et al., "Cholangiocarcinoma: current knowledge and future perspectives consensus statement from the European Network for the Study of Cholangiocarcinoma (ENS-CCA)," *Nature Reviews. Gastroenterology & Hepatology*, vol. 13, no. 5, pp. 261–280, 2016.

[20] S. Rizvi, S. A. Khan, C. L. Hallemeier, R. K. Kelley, and G. J. Gores, "Cholangiocarcinoma – evolving concepts and therapeutic strategies," *Nature Reviews. Clinical Oncology*, vol. 15, no. 2, pp. 95–111, 2018.

[21] X. Hu, Q. Pang, H. Liu et al., "Inflammation-based prognostic scores in patients with extrahepatic bile duct lesions treated by percutaneous transhepatic biliary stenting combined with (125)I seeds intracavitary irradiation," *Clinical & Translational Oncology*, vol. 21, no. 5, pp. 665–673, 2019.

[22] Q. Pang, L. Zhou, X. S. Hu et al., "Biliary stenting alone versus biliary stenting combined with 125I particles intracavitary irradiation for the treatment of advanced cholangiocarcinoma," *Scientific Reports*, vol. 9, no. 1, article 11348, 2019.

[23] H. W. Wang, X. J. Li, S. J. Li, J. R. Lu, and D. F. He, "Biliary stent combined with iodine-125 seed strand implantation in malignant obstructive jaundice," *World Journal of Clinical Cases*, vol. 9, no. 4, pp. 801–811, 2021.

[24] J. X. Ma, Z. D. Jin, P. R. Si et al., "Continuous and low-energy 125I seed irradiation changes DNA methyltransferases expression patterns and inhibits pancreatic cancer tumor growth," *Journal of Experimental & Clinical Cancer Research*, vol. 30, no. 1, p. 35, 2011.

[25] Z. Wang, Z. Zhao, J. Lu et al., "A comparison of the biological effects of 125I seeds continuous low-dose-rate radiation and 60Co high-dose-rate gamma radiation on non-small cell lung cancer cells," *PLoS One*, vol. 10, no. 8, article e0133728, 2015.

[26] A. R. Delbridge and A. Strasser, "The BCL-2 protein family, BH3-mimetics and cancer therapy," *Cell Death and Differentiation*, vol. 22, no. 7, pp. 1071–1080, 2015.

[27] L. M. Brown, D. T. Hanna, S. L. Khaw, and P. G. Ekert, "Dysregulation of BCL-2 family proteins by leukemia fusion genes," *The Journal of Biological Chemistry*, vol. 292, no. 35, pp. 14325–14333, 2017.

[28] A. Qu, H. Wang, J. Li et al., "Biological effects of (125)i seeds radiation on A549 lung cancer cells: G2/M arrest and enhanced cell death," *Cancer Investigation*, vol. 32, no. 6, pp. 209–217, 2014.

[29] M. Shariati and F. Meric-Bernstam, "Targeting AKT for cancer therapy," *Expert Opinion on Investigational Drugs*, vol. 28, no. 11, pp. 977–988, 2019.

[30] J. Liu, H. Wang, A. Qu, J. Li, Y. Zhao, and J. Wang, "Combined effects of C225 and 125-iodine seed radiation on colorectal cancer cells," *Radiation Oncology*, vol. 8, no. 1, p. 219, 2013.

[31] C. Liu, L. Wang, H. Qiu et al., "Combined strategy of radioactive 125I seeds and salinomycin for enhanced glioma chemoradiotherapy: evidences for ROS-mediated apoptosis and signaling crosstalk," *Neurochemical Research*, vol. 43, no. 7, pp. 1317–1327, 2018.

[32] J. H. Rong, D. Li, and Y. L. Li, "Lobaplatin enhances radioactive 125I seed-induced apoptosis and anti-proliferative effect in non-small cell lung cancer by suppressing the AKT/mTOR pathway," *Oncotargets and Therapy*, vol. 14, pp. 289–300, 2021.